MAR 1 6 1998 **ORNL-6930**

ornl

OAK RIDGE NATIONAL LABORATORY

LOCKHEED MARTIN

Durability-Based Design Criteria for an Automotive Structural Composite: Part 1. Design Rules

J. M. Corum
R. L. Battiste
C. R. Brinkman
W. Ren
M. B. Ruggles
G. T. Yahr

MANAGED AND OPERATED BY
LOCKHEED MARTIN ENERGY RESEARCH CORPORATION
FOR THE UNITED STATES
DEPARTMENT OF ENERGY

ORNL-27 (3-96)

This report has been reproduced directly from the best available copy.

Available to DOE and DOE contractors from the Office of Scientific and Technical Information, P.O. Box 62, Oak Ridge, TN 37831; prices available from (423) 576-8401.

Available to the public from the National Technical Information Service, U.S. Department of Commerce, 5285 Port Royal Rd., Springfield, VA 22161.

This report was prepared as an account of work sponsored by an agency of the United States Government. Neither the United States Government nor any agency thereof, nor any of their employees, makes any warranty, express or implied, or assumes any legal liability or responsibility for the accuracy, completeness, or usefulness of any information, apparatus, product, or process disclosed, or represents that its use would not infringe privately owned rights. Reference herein to any specific commercial product, process, or service by trade name, trademark, manufacturer, or otherwise, does not necessarily constitute or imply its endorsement, recommendation, or favoring by the United States Government or any agency thereof. The views and opinions of authors expressed herein do not necessarily state or reflect those of the United States Government or any agency thereof.

ORNL-6930

Engineering Technology Division

DURABILITY-BASED DESIGN CRITERIA FOR AN AUTOMOTIVE STRUCTURAL COMPOSITE: PART 1. DESIGN RULES

J. M. Corum
R. L. Battiste
C. R. Brinkman
W. Ren
M. B. Ruggles
G. T. Yahr

February 1998

Prepared by the
OAK RIDGE NATIONAL LABORATORY
Oak Ridge, Tennessee 37831-6285
managed by
LOCKHEED MARTIN ENERGY RESEARCH CORP.
for the
U.S. DEPARTMENT OF ENERGY
under contract DE-AC05-96OR22464

CONTENTS

PART 1: DESIGN RULES

	Page
LIST OF FIGURES	ix
LIST OF TABLES	xi
PREFACE	xv
ABSTRACT	1-1
1. INTRODUCTION	1-1
1.1 GENERAL	1-1
1.2 REFERENCE MATERIAL	1-2
1.3 LOADINGS AND ENVIRONMENTS	1-2
1.4 DESIGN APPROACH	1-2
1.5 DEFINITIONS	1-3
2. DEFORMATION AND STIFFNESS PROPERTIES FOR DESIGN ANALYSES	2-1
2.1 GENERAL	2-1
2.2 ELASTIC CONSTANTS FOR DESIGN	2-1
2.2.1 Basic Values	2-1
2.2.2 Environmental Effects	2-2
2.2.3 Prior Loading Effects	2-3
2.3 CREEP BEHAVIOR FOR DESIGN	2-3
2.3.1 Basic Creep Equation	2-3
2.3.2 Isochronous Stress-Strain Curves	2-6
2.3.3 Environmental Effects	2-6
3. MULTIAXIAL STRENGTH CRITERION — EQUIVALENT STRESS	3-1
4. DESIGN ALLOWABLES FOR STATIC LOADINGS	4-1
4.1 SHORT-TIME ALLOWABLE STRESS INTENSITY, S_0	4-1
4.2 TIME-DEPENDENT ALLOWABLE STRESS INTENSITY, S_t	4-2
4.3 TREATMENT OF INCREMENTS OF SUSTAINED LOADS	4-6
5. DESIGN LIMITS FOR CYCLIC LOADINGS	5-1
5.1 BASIC FATIGUE DESIGN CURVES	5-1
5.2 TREATMENT OF MEAN STRESSES	5-2
5.3 ENVIRONMENTAL EFFECTS	5-2
5.4 TREATMENT OF VARYING STRESS AMPLITUDES	5-4
5.5 FATIGUE EVALUATION PROCEDURE	5-4
6. DAMAGE TOLERANCE DESIGN FOR LOW-ENERGY IMPACTS AND OTHER DEFECTS	6-1
6.1 GENERAL REQUIREMENTS	6-1
6.2 DETERMINATION OF DAMAGE AREA	6-1
6.3 DETERMINATION OF STRENGTH AND STIFFNESS DEGRADATION	6-1
7. SUMMARY—SIMPLIFIED CRITERIA	7-1
7.1 STIFFNESS AND CREEP PROPERTIES FOR DESIGN ANALYSES	7-1
7.2 MULTIAXIAL STRENGTH THEORY	7-2
7.3 ALLOWABLE STRESSES FOR STATIC LOADINGS	7-2
7.4 LIMITS FOR CYCLIC LOADINGS	7-3
7.5 DAMAGE TOLERANCE EVALUATION	7-4

CONTENTS

PART 2: BACKGROUND DATA AND MODELS

	Page
LIST OF FIGURES	ix
LIST OF TABLES	xiii
ABSTRACT	1-1
1. INTRODUCTION	1-1
1.1 BACKGROUND	1-1
1.2 REFERENCE COMPOSITE	1-2
1.3 OVERVIEW OF PART 1 RULES	1-2
1.4 OVERVIEW OF PART 2	1-2
2. ELASTIC ANALYSIS	2-1
3. TENSILE, COMPRESSIVE, AND FLEXURAL ELASTIC CONSTANTS AND STRENGTH PROPERTIES	3-1
3.1 IN-AIR ELASTIC CONSTANTS AND STRENGTH PROPERTIES AS A FUNCTION OF TEMPERATURE	3-1
3.1.1 Tensile Elastic Constants and Strength Properties	3-1
3.1.2 Compressive Elastic Constants and Strength Properties	3-5
3.1.3 Flexural Elastic Constants and Strength Properties	3-6
3.2 PROPORTIONAL LIMIT, STRENGTH VALUES, AND DAMAGE DEVELOPMENT IN TENSILE LOADING	3-6
3.3 EFFECT OF STRAIN RATE	3-8
4. IN-PLANE AND INTERLAMINAR SHEAR PROPERTIES	4-1
4.1 IN-PLANE SHEAR MODULUS AND STRENGTH	4-1
4.2 INTERLAMINAR SHEAR	4-1
4.3 ENVIRONMENTAL DEGRADATION	4-3
4.4 OBSERVATIONS AND RECOMMENDATIONS	4-3
5. ENVIRONMENTAL DEGRADATION OF STRENGTH AND STIFFNESS	5-1
5.1 CORRELATIONS OF EFFECTS OF MOISTURE EXPOSURE ON STRENGTH AND STIFFNESS	5-1
5.2 FACTORS FOR OTHER FLUIDS	5-7
6. MULTIAXIAL STRENGTH CRITERION	6-1
7. REPRESENTATION OF CREEP UNDER VARIOUS STRESS, TEMPERATURE, AND ENVIRONMENTAL CONDITIONS	7-1
7.1 INTRODUCTION	7-1
7.2 REFERENCE CREEP EQUATION	7-1
7.3 TEMPERATURE DEPENDENCE	7-4
7.4 EFFECT OF DISTILLED WATER ON CREEP (ROOM TEMPERATURE)	7-10
7.5 EFFECTS OF OTHER ENVIRONMENTS ON CREEP	7-13
APPENDIX 7.A	7-15
APPENDIX 7.B	7-17
APPENDIX 7.C	7-19
8. DEVELOPMENT OF CREEP-RUPTURE CORRELATIONS AND DESIGN CURVES IN VARIOUS ENVIRONMENTS	8-1
8.1 INTRODUCTION	8-1
8.2 CREEP-RUPTURE CURVES AND EQUATIONS FOR VARIOUS TEMPERATURES IN AIR/50% RH	8-1
8.3 TABLE OF TIME/TEMPERATURE VALUES	8-12

8.4 DESIGN CURVES AND TABLE 8-12
8.4.1 In Air 8-12
8.4.2 In Distilled Water 8-15
8.4.3 Superimposed Motor Vibration and Low-Frequency Impulse Load Cycling on Creep-Rupture Strength 8-19
8.4.4 In Water-Based Fluids 8-22
8.4.5 In Oil-Based Fluids 8-23
8.4.6 In Sulfuric Acid Environment 8-23
8.5 ENVIRONMENTAL KNOCK-DOWN FACTORS 8-27
8.6 PROCEDURES FOR DEVELOPING CREEP-RUPTURE CURVES AND ALLOWABLE STRESSES 8-29
8.6.1 General Procedures and Precaution for Applications 8-29
8.6.2 Some Details in Developing the Maximum Design-Allowable Stress Curves 8-30
8.7 APPLICABILITY OF TIME FRACTIONS FOR CREEP-RUPTURE 8-32
9. ENVIRONMENTAL EFFECTS ON CREEP DEFORMATION AND RUPTURE DESIGN CURVES OF THE CSM ISOCYANURATE COMPOSITE FOR COMPRESSIVE LOADINGS 9-1
9.1 INTRODUCTION 9-1
9.2 CREEP DEFORMATION CURVES FOR AIR/50% RH AND DISTILLED WATER 9-1
9.2.1 Creep Deformation in Air/50% RH 9-1
9.2.2 Creep Deformation in Distilled Water 9-1
9.2.3 Loading Deformation 9-1
9.3 COMPRESSIVE CREEP-RUPTURE AND DESIGN CURVES IN AIR/50% RH AND WATER 9-11
9.3.1 Creep-Rupture Life and Creep-Rupture Strain 9-11
9.3.2 Creep Rupture and Design Curves and Equations 9-11
10. BASIC FATIGUE BEHAVIOR AND CORRELATIONS 10-1
10.1 INTRODUCTION 10-1
10.2 FATIGUE S-N CURVES 10-1
10.3 CYCLIC DAMAGE 10-3
10.4 DESIGN MARGINS 10-12
10.5 CONCLUSIONS 10-12
11. RECOMMENDED FATIGUE DESIGN 11-1
11.1 INTRODUCTION 11-1
11.2 FATIGUE DESIGN CURVES 11-1
11.3 ENVIRONMENTAL EFFECTS 11-1
11.4 TREATMENT OF MEAN STRESSES 11-6
11.5 TREATMENT OF CYCLES OF VARYING AMPLITUDES 11-8
11.6 SUMMARY 11-9
12. EFFECTS OF PRIOR STATIC, CYCLIC, AND SUSTAINED LOADINGS 12-1
12.1 INTRODUCTION 12-1
12.2 EFFECT OF PRIOR STATIC LOADING 12-1
12.3 EFFECT OF PRIOR FATIGUE CYCLES ON TENSILE PROPERTIES 12-1
12.4 EFFECT OF PRIOR FATIGUE CYCLES ON CREEP-RUPTURE STRENGTH 12-4
12.5 EFFECT OF PRIOR CREEP ON TENSILE STRENGTH AND STIFFNESS 12-6
12.6 SUMMARY 12-7
13. DAMAGE TOLERANCE DESIGN FOR IMPACTS 13-1
13.1 INTRODUCTION 13-1
13.2 BASIC IMPACT TESTS AND RESULTS 13-1
13.3 EFFECT ON TENSILE, COMPRESSIVE, AND FATIGUE PROPERTIES 13-3
13.4 BRICK-DROP TESTS 13-6
13.5 RECOMMENDED DESIGN APPROACH 13-7

14. SENSITIVITY TO STRESS CONCENTRATIONS—HOLES 14-1
14.1 INTRODUCTION 14-1
14.2 FINITE-ELEMENT ANALYSES 14-1
14.3 TENSILE TESTS 14-1
14.4 FATIGUE TESTS 14-1
14.5 CREEP-RUPTURE TESTS 14-4
14.6 SUMMARY 14-4
15. HAT SECTION FRACTURE TESTS—IMPLICATIONS FOR DESIGN CRITERIA 15-1
15.1 INTRODUCTION 15-1
15.2 MONOTONIC TESTS 15-1
15.3 APPLICATION OF DESIGN GUIDE 15-4
15.4 FATIGUE TESTS 15-4
15.5 SUMMARY 15-8
16. PREDICTIVE MODEL FOR TIME-DEPENDENT DEFORMATION 16-1
16.1 GENERAL 16-1
16.2 DATA AND MODEL 16-1
16.2.1 Linear Range ($0 \leq \sigma < 5.2$ ksi) 16-1
16.2.2 Nonlinear Range ($\sigma > 5.2$ ksi) 16-1
16.2.3 Temperature Effects 16-2
16.2.4 Effects of Distilled Water 16-2
16.2.5 Cyclic Loading 16-3
16.2.6 Generalizations 16-3
16.3 ISOCHRONOUS STRESS-STRAIN CURVES 16-4
16.4 DETAILED RESULTS 16-4
17. DAMAGE DEVELOPMENT AND GROWTH 17-1
17.1 INTRODUCTION 17-1
17.2 DAMAGE INITIATION 17-1
17.3 DAMAGE PROPAGATION 17-2
17.4 ENVIRONMENTAL EFFECTS 17-2

LIST OF FIGURES

Figure		Page
2.1	Multiplication factor for determining strength and stiffness at given temperature from room-temperature values	2-2
2.2	Creep curves and creep equation for room-temperature air/50% RH	2-4
2.3	Creep-strain multiplier for temperature effects	2-5
2.4	Isochronous stress-strain curves for room-temperature air/50% RH	2-6
3.1	Comparison of maximum shear stress criterion with average failure points in tension, biaxial tension, compression, and shear for reference composite	3-1
4.1	S_t values without environmental effects	4-3
4.2	S_t values with bounding environmental and prior loading effects	4-5
5.1	Design fatigue curves	5-1
5.2	Minimum creep-rupture stress values, S_T	5-3
6.1	Design curve for determining impact damage area	6-2
6.2	Calculated peak contact force vs damage area	6-3
6.3	Strength degradation as a function of damage area	6-4

LIST OF TABLES

Table		Page
2.1	Modulus of elasticity at various temperatures	2-2
2.2	Temperature multiplication factors for creep	2-6
2.3	Creep strain multipliers for immersion in various automotive environments	2-8
4.1	S_0 values at various temperatures	4-1
4.2	S_0 values degraded by environment and prior cyclic loading	4-2
4.3	Allowable stress intensity values, S_t (ksi) without environmental effects	4-2
4.4	Temperature and environmental effects on creep-rupture strength	4-4
4.5	Allowable stress intensity values, S_t (ksi) with bounding environmental and prior load effects	4-4
5.1	UTS at various temperatures	5-2
5.2	σ_r at 5000 h for use in modified Goodman relation	5-3
5.3	Fatigue stress-reduction factors for various automotive fluid environments	5-4
7.1	Temperature multipliers for modulus of elasticity	7-1
7.2	Time-dependent modulus values	7-1
7.3	Temperature multipliers for time-dependent moduli	7-2
7.4	S_t values expressed as multipliers on S_0 at room temperature	7-3
7.5	Maximum allowable cyclic stresses as a percent of UTS_{avg}	7-4
7.6	Predicted effect of low-energy impacts	7-4

CONVERSION FACTORS

U.S. Customary Units to SI Units

Quantity	Multiply	By	To obtain
Length	inch (in.)	2.54×10^{-2}	meter (m)
Force	pound (lb)	4.448	newton (N)
Stress	pound/inch^2 (psi)*	6.895×10^6	pascal (Pa)
Velocity	foot/second (ft/s)	0.3048	meter/second (m/s)
Temperature	temperature (°F – 32)	0.5556	temperature (°C)

*ksi = 10^3 psi; Msi = 10^6 psi.

PREFACE

It is hoped that this proposed design criteria document for a single candidate automotive structural composite will provide the nucleus for a full-scale design guide as additional composites are added and as guidance from composite designers is incorporated. Comments and suggestions for modifications and improvements are eagerly solicited. They should be sent to the following address:

J. M. Corum
Oak Ridge National Laboratory
Post Office Box 2009
Oak Ridge, Tennessee 37831-8051
Fax: 423/574-0740
Internet: jcp@ornl.gov

DURABILITY-BASED DESIGN CRITERIA FOR AN AUTOMOTIVE STRUCTURAL COMPOSITE: PART 1. DESIGN RULES

J. M. Corum, W. Ren, R. L. Battiste, M. B. Ruggles, C. R. Brinkman, and G. T. Yahr

ABSTRACT

This proposed durability-based design criteria document for an automotive structural composite is the result of a U.S. Department of Energy Advanced Automotive Materials project entitled "Durability of Lightweight Composite Structures." The overall goal of the project is to develop experimentally based, durability-driven design guidelines for automotive structural composites. The project is closely coordinated with the Automotive Composites Consortium (ACC). The initial reference material addressed by this document was chosen and supplied by ACC. The material is a structural reaction injection-molded isocyanurate (urethane), reinforced with continuous-strand, swirl-mat E-glass fibers.

The durability issues addressed include the effects of cyclic and sustained loadings, temperature, automotive fluid environments, vibrations, and low-energy impacts (e.g., tool drops and roadway kickups) on deformation, strength, and stiffness. This criteria document provides design analysis guidance, time-independent and time-dependent allowable stresses, rules for cyclic loading, and damage-tolerance design guidance. Environmental degradation factors and the degrading effects of prior loadings are included. A companion document, *Part 2: Background Data and Models* (ORNL-6931), provides the underlying experimental data and models for the reference composite.

Included in Part 2 is a chapter on static and fatigue tests of subscale components. These tests, and associated analyses, provided a means of assessing, and demonstrating the reasonableness of, several of the basic rules in Part 1. A more comprehensive design example is being planned in which a realistic component will be designed by the rules presented here and then structurally tested. The example will touch on most of the conditions covered by the rules.

It is anticipated that the design criteria framework presented here will be adaptable to other automotive structural composites, including those made by manufacturing processes other than liquid molding and containing reinforcements other than continuous-strand glass mats. Efforts are currently under way to generate the information to add two composites: one reinforced with chopped, directed glass fiber and one reinforced with carbon fiber.

1. INTRODUCTION

1.1 GENERAL

This durability-based design criteria document is intended to eventually apply to a variety of automotive structural composites—both glass- and carbon-fiber-reinforced. This initial version is based on, and is thus applicable to, a single reference material—a urethane reinforced with a glass-fiber continuous-strand mat (CSM). This reference material has been extensively characterized and modeled from a durability standpoint by the U.S. Department of Energy (DOE) project entitled "Durability of Lightweight Composite Structures for Automotive Applications" at the Oak Ridge National Laboratory (ORNL).

This Part 1 document provides detailed rules and guidelines for (1) the properties to be used in structural analyses, (2) design allowables for static loadings, (3) design rules for cyclic loadings, and (4) damage tolerance design for low-energy impacts. In each case, the range of automotive environments is taken into account. A final chapter condenses the more detailed rules into a simplified set of rules

consisting of knockdown factors applied to static properties. Both the detailed and simplified rules are intended to ensure the long-term (15-year) durability of automotive composite structures.

A companion document, P*art 2: Background Data and Models* (ORNL-6931), provides the durability information on which this Part 1 document is based. Part 2 includes 16 position papers (chapters), each covering key topics. Frequent reference is made here to those position papers by referring to the appropriate chapter of Part 2.

1.2 REFERENCE MATERIAL

The reference material is a structural reaction injection-molded (SRIM) isocyanurate (polyurethane) reinforced with continuous strand, swirl-mat E-glass. The isocyanurate resin is DOW MM364, and the reinforcement is Vetrotex Certainteed Unifilo U750. This initial reference material was chosen by the Automotive Composites Consortium (ACC) and supplied in the form of 25 × 25 × 1/8-in.-thick plaques. Five layers of mat were used in each plaque, resulting in a fiber content of about 25% by volume (40–50% by weight).

Although the CSM used in the reference material is intended to be nearly isotropic, the properties do vary (see Chap. 3 of Part 2). For example, the elastic modulus in the 0° direction (parallel to the roll direction of the original glass mat) is, on average, 18% less than the 90° value. Strengths vary in an analogous manner. Generally, values and allowables in this document are based on the weaker 0°-direction properties.

Chapter 17 of Part 2 contains a discussion of the observed damage development and growth process of the reference material under various loadings and environments.

1.3 LOADINGS AND ENVIRONMENTS

From a durability standpoint, it is assumed here that an automobile with a composite structure must last for 15 years (131,500 h) and 150,000 miles. It is further assumed that during the 15 years, the vehicle will actually be operated between 3000 and 5000 h (at an average speed of 30 to 50 mph).

The design temperature range is assumed to vary from a minimum of –40°F to a maximum of 250°F, with the higher temperatures occurring only during operation.

In addition to functional stiffness and deformation requirements, structures must support and resist a variety of live and dead loads. During operation, for example, live loads might include a combination of pothole impact, hard turn, and maximum acceleration. Dead loads during the 15-year life would include those from the weight of the vehicle or, more importantly, sustained loads in the bed of a light truck.

Structures will also be subjected to common vehicle fluids and operating atmospheres, and design limits must take the resulting property degradation into account. Fluids and atmospheres considered here include distilled water and saltwater, high-humidity air [>90% relative humidity (RH)], windshield washer fluid, engine coolant, motor oil, brake fluid, gasoline, and battery acid. In addition, motor vibrations were considered because they can degrade long-term creep properties.

Finally, composite automotive structures must be designed to resist damage from routine low-energy impacts, such as roadway kickups, tool drops, and, in the case of a pickup box, dropped bricks and cattle hooves.

1.4 DESIGN APPROACH

It is assumed that design analyses will primarily be elastic finite-element plate and shell analyses providing, in addition to deformations, normal membrane and bending stresses plus shear in the relatively thin molded sections. Chapter 2 provides the required elastic constants for analysis, including the degrading effects of environments and prior loadings. Chapter 2 also provides a creep equation, together with factors to account for temperature and environment, and references to a constitutive model that can be used to predict time-dependent creep and recovery. More practicably, pseudo-time-dependent modulus values are provided for use in simplified elastic analyses for approximately predicting creep deformations.

1.5 DEFINITIONS

E	Elastic modulus
E_t	Time-dependent "pseudo elastic modulus"
F	Maximum indentation force during an impact
G	Shear modulus [$E = 2G(1 + \nu)$ for an isotropic material]
m	Mass of impacting object
n	Number of applied fatigue cycles of a given stress
N_d	Number of allowable design cycles for a given stress
P	Calculated membrane stress components at a point in the plane of a plate or shell structure
Q	Calculated bending stress components at a point
R	Ratio of minimum to maximum stress in a fatigue cycle
S	Maximum stress intensity derived from stress components at a point (algebraically maximum minus algebraically minimum principal stress)
SCF	Stress concentration factor
S_r	Minimum creep-rupture strength at a given time
S_0	Basic short-time allowable stress intensity (time $t = 0$)
S_t	Time-dependent allowable stress intensity
t	Time at a given stress
T_d	Allowable design time at a given stress
UTS	Ultimate tensile strength
v	Velocity of impacting object
σ	Normal stress
σ_r	Average creep-rupture strength at a given time
σ_a	Stress amplitude in a fatigue cycle
σ_m	Mean stress in a fatigue cycle
σ_o	Stress amplitude in a completely reversed fatigue cycle
ν	Poisson's ratio
α	Indentation during an impact

2. DEFORMATION AND STIFFNESS PROPERTIES FOR DESIGN ANALYSES

2.1 GENERAL

The properties of the CSM reinforcing used in the reference composite are intended to be nominally isotropic in the plane of the mat. Manufacturing variables, however, resulted in fewer fibers oriented in the direction of the roll (0° direction) than transverse to it (90° direction). To accentuate this anisotropy in the reference composite plaques, the mat layers were oriented so that the weaker 0° directions coincided. As a result, all of the properties—stiffness, strength, fatigue, and creep—vary from the 0° to 90° direction. As stated in the previous chapter, the 0° elastic modulus is, on average, 18% less than the 90° value.

In this criteria document, the composite is treated as isotropic in the plane of the plaque. Further, the weaker 0° values are assumed to apply.

For an orthogonally anisotropic material that is isotropic in one plane, there are five independent elastic constants—two associated with the plane of the isotropy and three associated with the direction normal to that plane (see Chap. 2 of Part 2). In this case, the in-plane constants are taken as the modulus of elasticity, E, and Poisson's ratio, ν. The in-plane shear modulus, G, is then given by

$$G = \frac{E}{2(1 + \nu)} .$$

The other three constants are associated with the direction transverse to the plane of the plaque and are an E, G, and ν value.

At room temperature, the in-plane values are taken to be E = 1.37 Msi , and $\nu = 0.31$. These result in a calculated in-plane G value of 0.52 Msi.

As long as the stresses in the transverse direction (normal to the plane of the composite) are ignored, as they are in thin plate and shell analyses, only the in-plane properties are required. It should be realized, however, that this simplification does affect the accuracy of predicted transverse deformations (thickness changes). Also, although using only elastic properties for the weaker 0° direction will result in conservative deformation predictions for load-controlled situations, predicted stresses in deformation-controlled situations (e.g., discontinuity stresses, thermal stresses) may be unconservative.

2.2 ELASTIC CONSTANTS FOR DESIGN

2.2.1 Basic Values

The recommended average room-temperature elastic modulus, E, value for design with the reference composite is 1.37 Msi, and Poisson's ratio is 0.31. While Poisson's ratio is considered to be constant with temperature, E varies linearly according to the multiplication factor in Fig. 2.1. Values of E at various temperatures over the automotive design range are given in Table 2.1. These values may need to be reduced in accordance with the following two subsections.

The stiffness values in Table 2.1 are from tensile tests. Although compressive stiffness values are the same as tensile values at room temperature, compressive values drop much faster with increasing temperature than do tensile values (the same is true of compressive strength). These observations dictate that a part adjacent to a major heat source should not be in compression or, if it is, that it be provided with a heat shield or other form of heat protection.*

*See the following reference for information on the effects of temperature on properties of a urethane resin composite: D. Q. Houston and C. F. Johnson, "Correlating Composite Environmental Testing to Service," pp. 249–257 in *Advanced Composite Materials: New Developments and Applications Conference Proceedings*, Detroit, Sept. 30–Oct. 3, 1991.

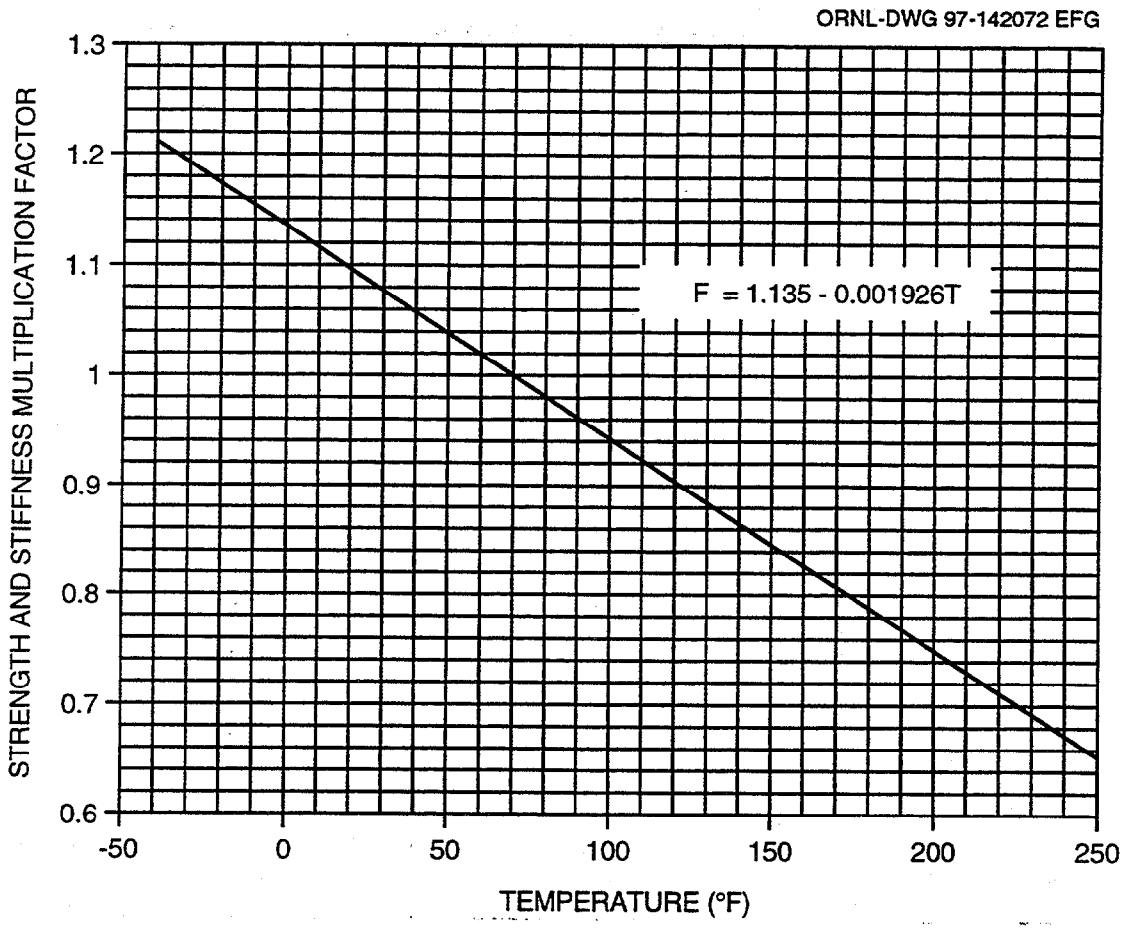

Fig. 2.1. Multiplication factor for determining strength and stiffness at given temperature from room-temperature values.

Table 2.1. Modulus of elasticity at various temperatures

Temperature (°F)	Factor	E (Msi)
–40	1.21	1.66
70	1.00	1.37
135	0.88	1.21
190	0.77	1.05
250	0.65	0.89

2.2.2 Environmental Effects

Chapter 5 of Part 2 presents data on the effects of moisture and other fluids on stiffness. A stiffness loss of 17% is recommended to bound environmental effects. The value is based on the following equation that gives the percentage loss in stiffness and ultimate tensile strength (UTS) following a water soak at room temperature for a given time, t, in hours.

$$\text{Percentage loss} = 3.44 \log_{10} t + 3.44 \ . \tag{2.1}$$

A 17% loss corresponds to 1 year (8760 h).

The 17% value is thought to adequately cover moisture effects, even under design loads. It should also adequately cover the effects of other fluids, including battery acid, for soak times up to 6 months.

2.2.3 Prior Loading Effects

Prior loadings can produce internal microstructural damage that is manifest as a reduction in stiffness. Data on these reductions are presented in Chap. 12 of Part 2. The findings reviewed there are summarized below.

- A single tensile loading to 0.67 UTS, which is the specified design allowable, produces a stiffness reduction on subsequent loading of 6.9%.
- Fatigue cycling to 5% of cyclic life, which is the specified design limit (design margin of 20 on cycles to failure), produces a stiffness loss of 10% or less.
- Prior creep does not reduce subsequent stiffness.

On the basis of these findings, it is recommended that a 10% stiffness reduction be used to account for prior loadings.

2.3 CREEP BEHAVIOR FOR DESIGN

In the case of long-term sustained loadings—either those associated with the 3000- to 5000-h operating life of an automobile or the 15-year overall life—creep deformations may become important and need to be accounted for in design analyses. This can be done at one of three levels of sophistication:

- using a time-dependent "pseudo-elastic modulus" in an elastic analysis,
- using a creep equation in an inelastic analysis, or
- using an appropriate constitutive model derived for the material that can predict the effects of changing load levels as well as recovery strains upon unloading.

Guidance for each is given here and in Part 2.

2.3.1 Basic Creep Equation

The average time-dependent creep response (loading strain subtracted out) of the reference composite at room temperature in air at 50% RH is reasonably well represented by the following creep equation (see Chap. 7 of Part 2):

$$\varepsilon^c = (0.00507\ \sigma)\ t^{0.196} \ , \tag{2.2}$$

where

$\varepsilon^c =$ creep strain (%),
$\sigma =$ applied stress (ksi),
$t =$ time (h).

This relation is linear in stress and holds reasonably well up to a stress of 14 ksi.* Figure 2.2 shows the creep curves predicted by Eq. (2.2). These curves are good for both tensile and compressive creep.

*As shown in Chap. 16 of Part 2, the creep response starts to depart slightly from linearity at a stress less than 6 ksi. The linear assumption used in Eq. (2.2) is thought, however, to be adequate for design.

ORNL-DWG 97-142073 EFG

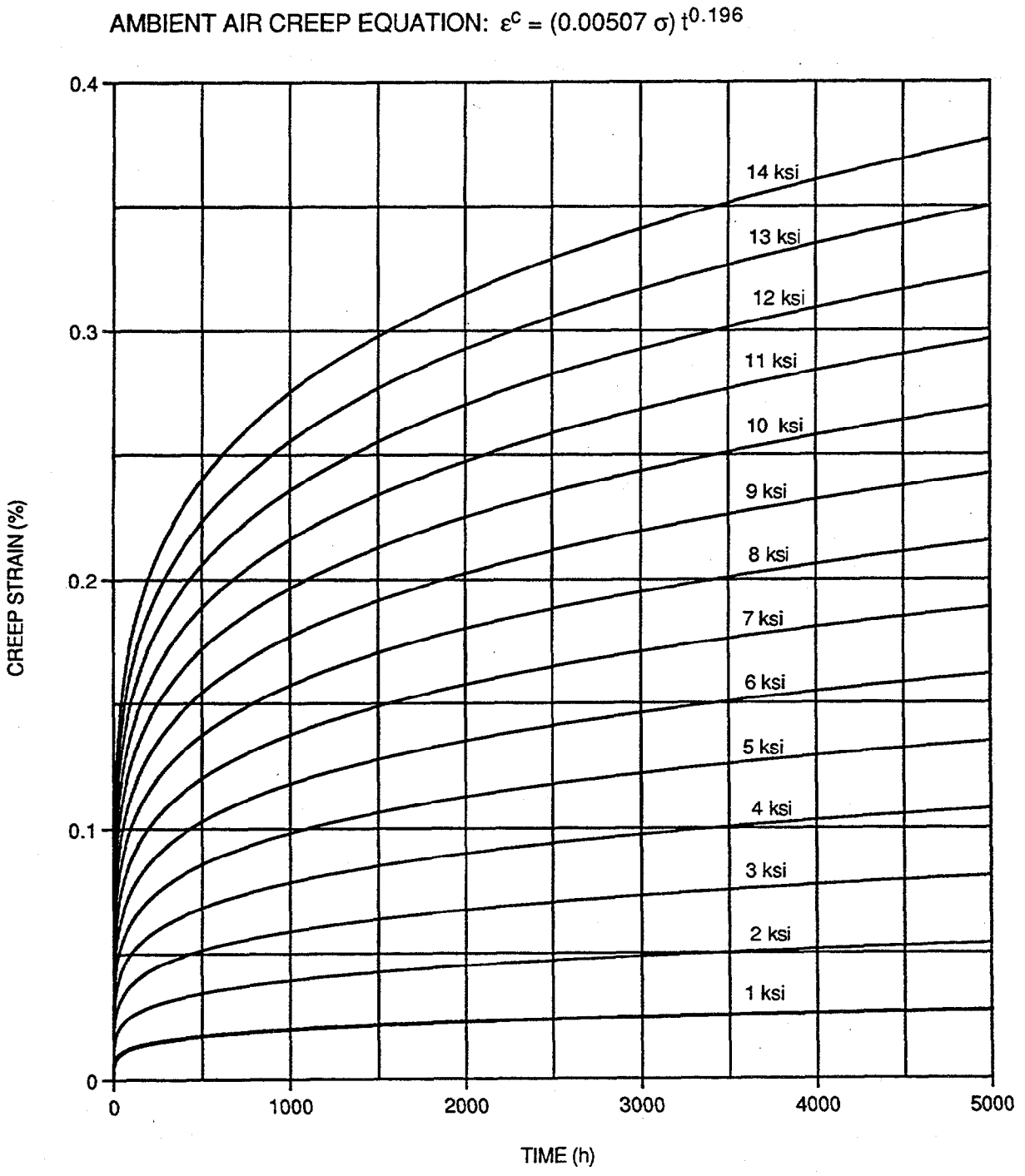

Fig. 2.2. Creep curves and creep equation for room-temperature air/50% RH.

The effect of temperature on creep is to multiply the creep strains predicted by Eq. (2.2) by a simple factor, which is shown in Fig. 2.3 for the automotive design temperature range and given in Table 2.2 for selected temperatures.

The adjusted creep equation is limited to the following maximum stresses:

Temperature (°F)	Maximum stress (ksi)
≤75	14
135	12
190	10
250	7.5

Note that while tensile and compressive creep are equal at room temperature, compressive creep becomes larger at elevated temperatures. No in-air data are available, but tests at higher stresses (11 and 12 ksi) in distilled water at 135°F show compressive creep strains up to twice those in tension.

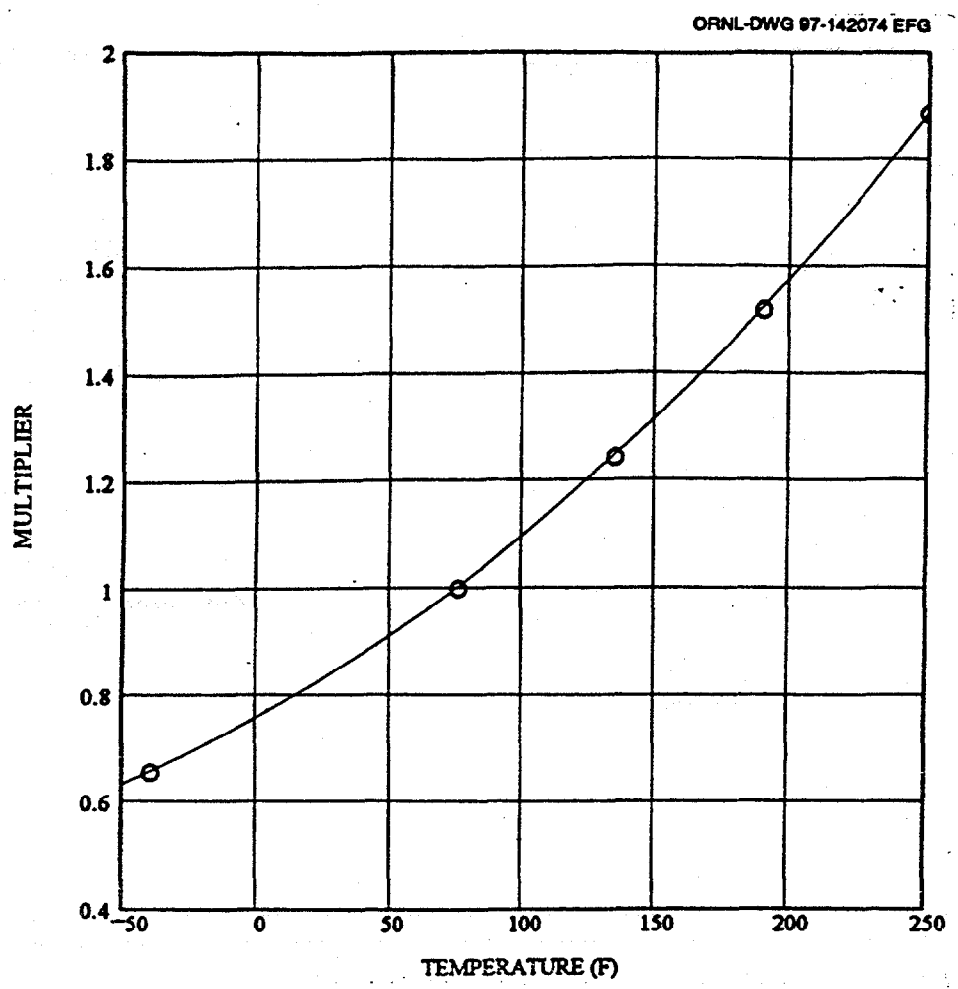

Fig. 2.3. Creep-strain multiplier for temperature effects.

Table 2.2. Temperature multiplication factors for creep

Temperature (°F)	Creep factor
–40	0.65
75	1.00
135	1.24
190	1.52
250	1.88

2.3.2 Isochronous Stress-Strain Curves

Isochronous stress-strain curves, which show the total strain at a given time corresponding to a constant applied stress, are often used to approximately predict creep effects. Although not rigorous, an isochronous curve for a given time can often be used in an elastic-plastic analysis to predict creep deformations reasonably well. Isochronous curves, for this purpose, are given in Fig. 2.4. An equation is also provided.

Because creep is linear with stress at the lower stress levels, the isochronous curves exhibit a "pseudo-elastic" region. The slopes of these linear regions can be viewed as time-dependent moduli and used in elastic analyses to approximately predict creep effects. Values of these time-dependent moduli, E_t, are tabulated in the inset of Fig. 2.4.

2.3.3 Environmental Effects

Chapter 7 of Part 2 develops multipliers on creep strain that, in a manner similar to the temperature multipliers, can be used to estimate the enhanced creep because of submersion in various automotive fluids. In all cases, the factors were derived from tests in which specimens were preconditioned for 100 h and then tested in the fluid of interest. The factors are given in Table 2.3.

A factor of 1.6 adequately covers all cases except battery acid and is recommended for design use. Use of this factor with the creep equation is limited to stresses of 8 ksi and below.

Note that the inverse of this creep strain multiplier (0.63) can be used conservatively as a multiplier on the time-dependent moduli tabulated in Fig. 2.4.* Likewise, the inverse of the temperature factor given in Sect. 2.3.1 can be conservatively used for E_t.

Another automotive environmental effect that has been explored is motor vibration superimposed on steady creep loads. Although these superimposed vibrations shorten creep-rupture life (see Chap. 8 of Part 2), they have not been found to affect creep deformations. Thus, no multiplying factor is needed for motor vibrations.

*The time-dependent moduli are given by $E_t = E\,E_c/(E + E_c)$, where E is the time-independent elastic modulus and E_c is the time-dependent creep modulus. As described in Sect. 2.2.2, the multiplier on E is 0.83. Use of the single factor, 0.63, is conservative. Alternatively, the two separate factors can be used with the above formula.

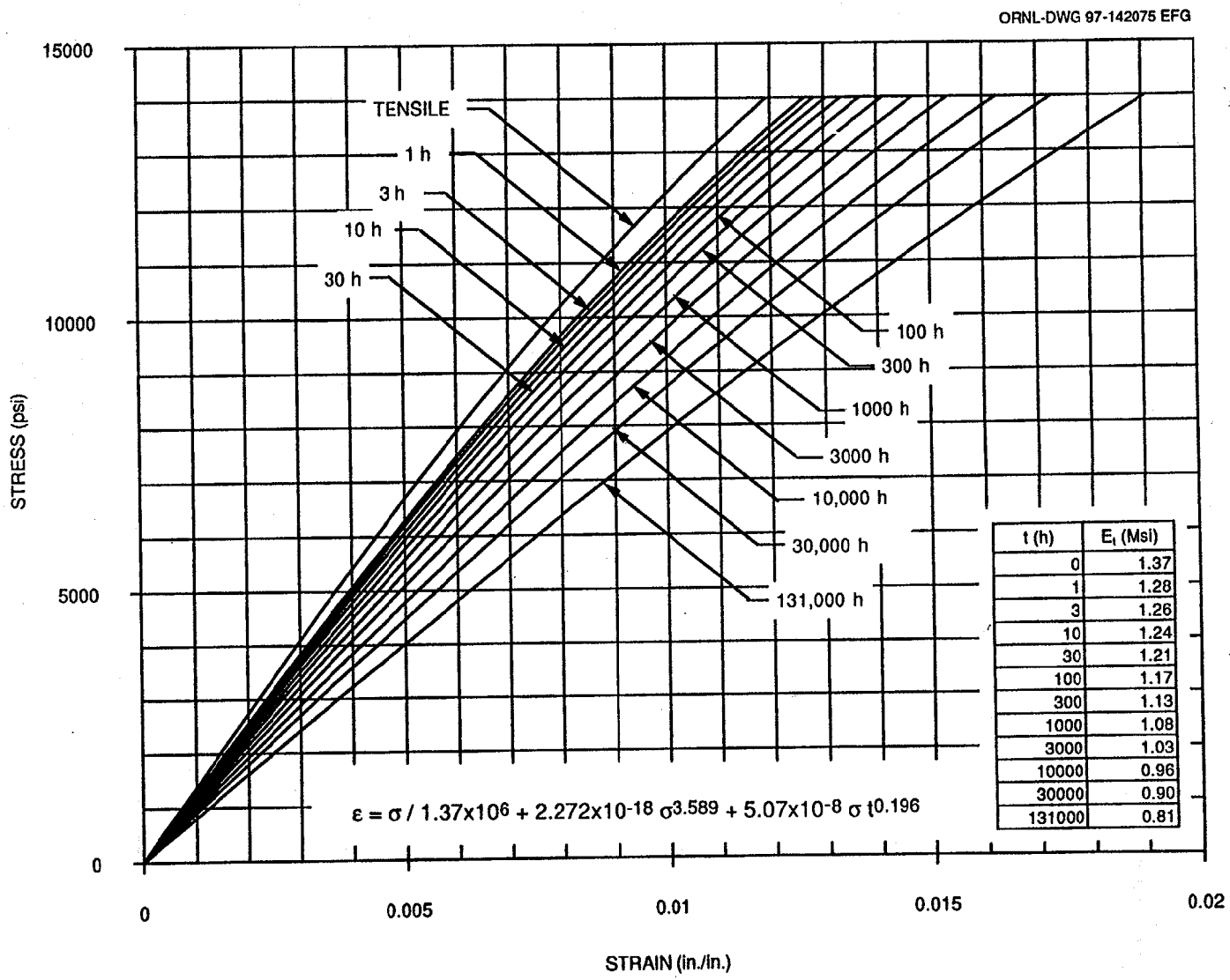

t (h)	E_t (Msi)
0	1.37
1	1.28
3	1.26
10	1.24
30	1.21
100	1.17
300	1.13
1000	1.08
3000	1.03
10000	0.96
30000	0.90
131000	0.81

Fig. 2.4. Isochronous stress-strain curves for room-temperature air/50% RH.

Table 2.3. Creep-strain multipliers for immersion in various automotive environments

Environment	Multiplier on creep strain
Distilled water	1.60
Motor oil	1.05
Brake fluid	1.30
Windshield wash	1.50
Saltwater	1.50
>90% RH	1.55
Battery acid	1.65

3. MULTIAXIAL STRENGTH CRITERION— EQUIVALENT STRESS

The allowable design limits recommended here are stress based. For design it is convenient to have a single equivalent quantity representing the multiaxial stress state at a point in the structure and time in the loading history. The equivalent stress used here is the stress intensity, S.

The equivalent intensity of combined stresses, or stress intensity, is defined as twice the maximum shear stress and is equivalent to the difference between the algebraically largest principal stress and the algebraically smallest principal stress at a given point. Tensile stresses are considered positive, and compressive stresses are considered negative.

The stress intensity is based on the maximum shear stress theory of failure, which, for the reference composite, has been shown to conservatively describe multiaxial failure conditions (see Chap. 6 of Part 2). Figure 3.1 shows average failure points in tension, compression, and in-plane shear for the reference

ORNL-DWG 97-142076 EFG

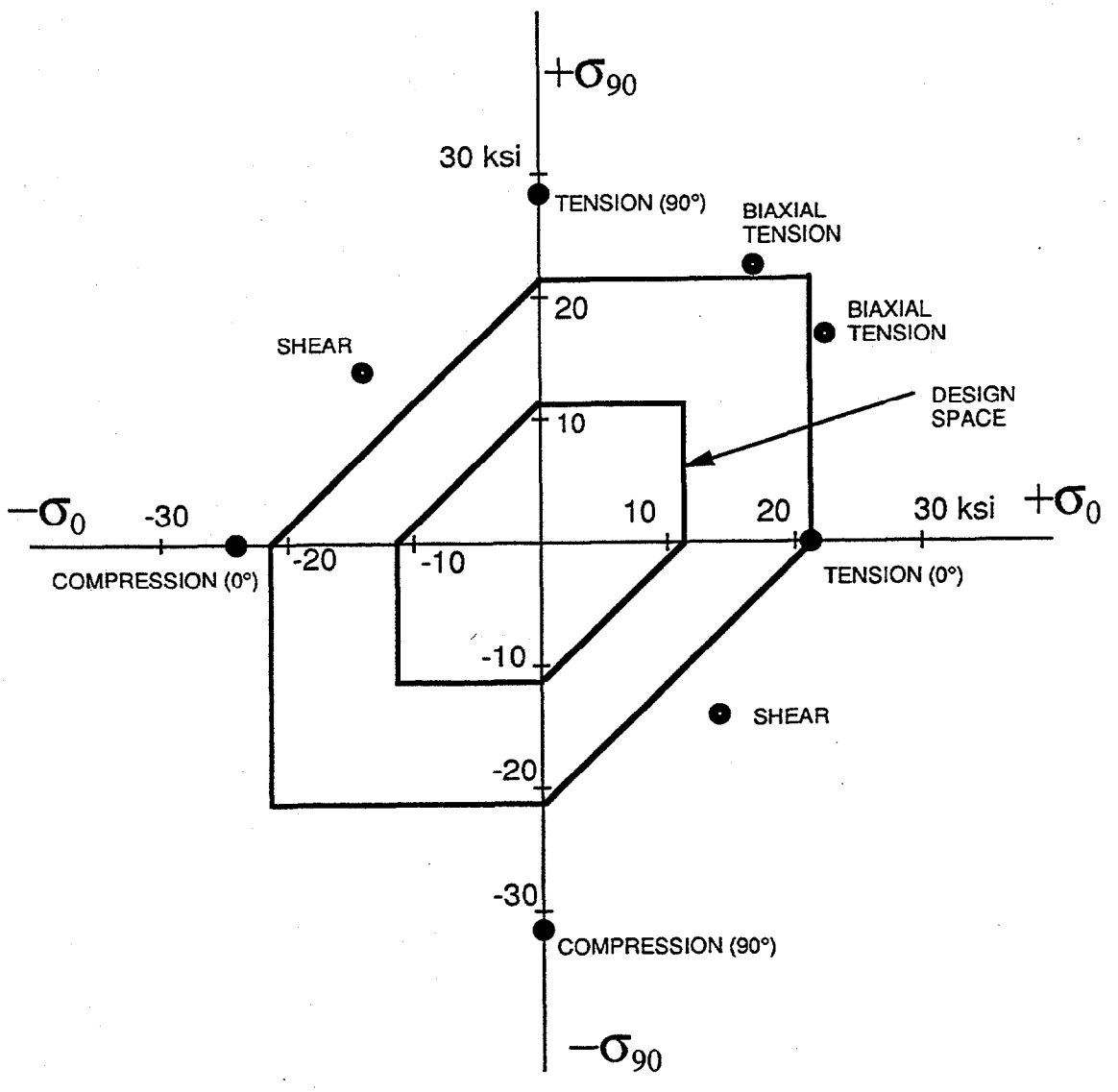

Fig. 3.1. Comparison of maximum shear stress criterion with average failure points in tension, biaxial tension, compression, and shear for the reference composite.

material. Also shown is the maximum shear stress criterion passing through the average uniaxial tensile strength in the weaker 0° direction. The criterion conservatively predicts all the other failure points. Thus, limiting the calculated stress intensity to an allowable uniaxial tensile stress (derived from the weaker 0° direction) ensures that compressive and shear stresses also do not exceed their respective limits.

The area labeled "design space" in Fig. 3.1 is based on an allowable stress that is two-thirds of the minimum UTS. This design margin is discussed in Chap. 4.

The maximum shear stress criterion is assumed to conservatively apply to fatigue and creep rupture as well. Thus, the stress intensity, previously defined, is used for evaluating sustained and cyclic loadings as well as short-time loads. Compressive fatigue tests show a strength higher than for tension at room temperature (see Chap. 11 of Part 2). Likewise, compressive creep-rupture strength at room temperature is equal to tensile strength (see Chap. 9 of Part 2). No shear or combined stress-state fatigue or creep-rupture data exist, however.

4. DESIGN ALLOWABLES FOR STATIC LOADINGS

4.1 SHORT-TIME ALLOWABLE STRESS INTENSITY, S_0

The basic short-time allowable stress intensity used here is based on the minimum UTS in the weaker 0° direction. This minimum room-temperature value for the reference composite is based on statistical treatment of the 185 0° UTS values, reported in Chap. 3 of Part 2, such that the survival probability is 90% at a confidence level of 95%. This is the "B-basis stress" used in MIL-HDBK-17.[1] Assuming a normal distribution, the minimum is defined as

$$UTS_{min} = UTS_{avg} - K(SD) \ , \tag{4.1}$$

where SD is the sample standard deviation and K = 1.457 for a population of 185, the number of 0° tensile tests reported in Chap. 3 of Part 2. The resulting room-temperature values are

$$UTS_{avg} = 21.3 \text{ ksi},$$

$$SD = 2.67 \text{ ksi, and}$$

$$UTS_{min} = 17.4 \text{ ksi}.$$

The basic time-independent allowable stress intensity, S_0, is defined as two-thirds UTS_{min}. At room temperature, S_0 thus becomes $S_0 = 11.6$ ksi.

Values for other temperatures are obtained by using the multiplier previously given for both stiffness and strength in Fig. 2.1. Values for S_0 at various temperatures are given in Table 4.1.

For environmental effects, the same 17% reduction recommended in Chap. 2 for stiffness holds for strength.* For the effects of prior loads, only cyclic loadings reduce subsequent strength. That reduction is limited to 1.5% with the design factor of 20 that is used on cycles (see Chap. 12 of Part 2). Taken together, environmental effects and prior cyclic loadings reduce S_0 to the values shown in Table 4.2.

Table 4.1. S_0 values at various temperatures

Temperature (°F)	S_0 (ksi)
–40	14.1
20	12.7
70	11.6
135	10.2
190	8.9
250	7.6

*Chapters 4 and 5 of Part 2 indicate that environmental degradation in compression and shear is no worse than in tension at room temperature. Thus, the degraded S_0 values given in Table 4.2 are believed to cover all stress states at normal temperatures.

Table 4.2. S_0 values degraded by environment and prior cyclic loading

Temperature (°F)	S_0 (ksi)
–40	11.5
20	10.4
70	9.5
135	8.3
190	7.4
250	6.2

4.2 TIME-DEPENDENT ALLOWABLE STRESS INTENSITY, S_t

For time-dependent loadings, creep-rupture stress is the basis for allowable stresses, provided that S_0 is not lower than the creep-rupture-derived values. The following design margin is used:

$$0.8\, S_r \ ,$$

where S_r is the minimum creep-rupture strength.

For the reference composite, minimum tensile creep-rupture values were determined as described and reported in Chap. 8 of Part 2. Compressive creep-rupture strengths are equal to tensile strength values at room temperature. No elevated-temperature, in-air compressive creep-rupture results are available. However, at elevated temperatures in water, the compressive values are less (see Chap. 9 of Part 2).

A time-dependent allowable stress intensity, S_t, is defined as

$$S_t \leq \begin{cases} S_0 \\ 0.8\, S_r \end{cases} . \tag{4.2}$$

Values of S_t without environmental effects are tabulated in Table 4.3 and plotted in Fig. 4.1. Values are truncated at 5000 h when they are associated only with operating conditions. The creep-rupture based values in Table 4.3 were obtained from Table 8.2 in Chap. 8 of Part 2 by multiplying the normalized values there by 21.3 ksi, the average room-temperature UTS.

Table 4.3. Allowable stress intensity values, S_t (ksi) without environmental effects

Temperature (°F)	Time						
	0 h	10 h	1000 h	3000 h	5000 h	1 year	15 years
–40	14.1	11.9	11.1	10.9	10.8	10.7	10.3
20	12.7	11.9	11.1	10.9	10.8	10.7	10.3
70	11.6	11.6	11.1	10.9	10.8	10.7	10.3
135	10.2	10.2	10.2	10.2	10.1	10	9.6
190	9	9	9	8.8	8.7		
250	7.6	6.8	6.0	5.9	5.8		

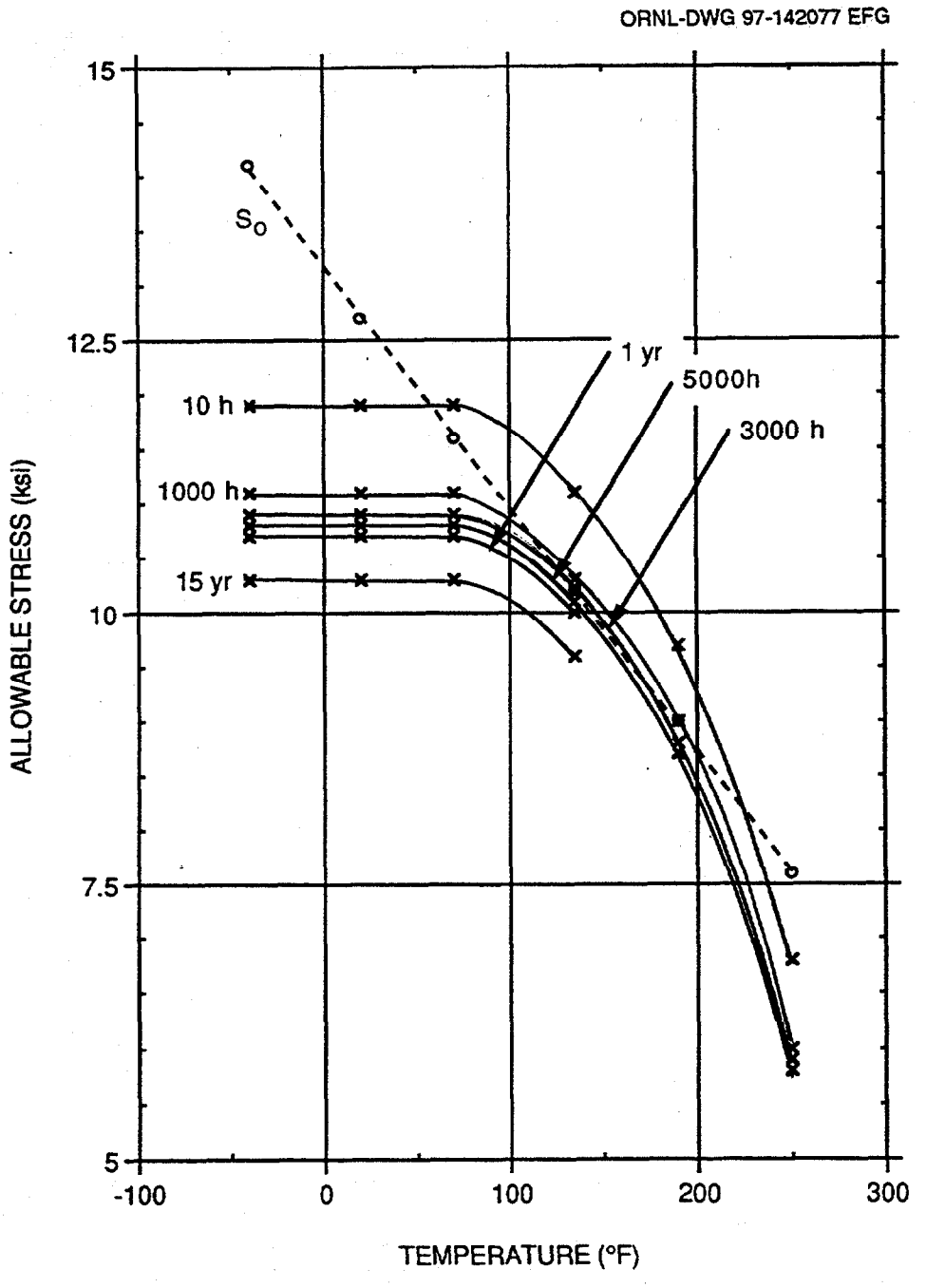

Fig. 4.1. S_t values without environmental effects.

The effects of temperature and environment on creep-rupture strength are given by the stress multipliers in Table 4.4 (see Chap. 8 of Part 2). Use of the shaded values (for tensile creep rupture in 135°F distilled water), with 0.51 used for 1 year and 15 years, bounds everything but battery acid and three hot water cases. Values of S_t with the shaded environmental degradation values incorporated are tabulated in Table 4.5 and plotted in Fig. 4.2. The time-dependent values in this figure and table are reduced by an additional 3% to account for the maximum effect of prior cyclic loads (see Chap. 12 of Part 2).

Table 4.4. Temperature and environmental effects on creep-rupture strength (Factors for conditions associated with operation are truncated at 5000 h)

Environment[a]	Time					
	10 h	1000 h	3000 h	5000 h	1 year	15 years
Room-temperature air/50% RH (T and C)	1	1	1	1	1	1
20°F air	1	1	1	1	1	1
135°F air	0.99	0.99	0.99	0.99	0.99	0.99
190°F air	0.91	0.91	0.91	0.91		
250°F air	0.66	0.65	0.65	0.64		
Room-temperature air/<10% RH	1	1	1	1	1	1
Room-temperature air/>90% RH	0.86	0.68	0.65	0.63	0.61	0.53
Room-temperature distilled water (T and C), saltwater, windshield wash, engine coolant	0.62	0.54	0.52	0.51		
135°F distilled water (T)	0.61	0.53	0.52	0.51		
135°F distilled water (C)	0.53	0.41	0.38	0.37		
190°F distilled water (T)	0.31	0.19	0.17	0.16		
190°F distilled water (C)	0.12	0.05	0.05	0.04		
Motor vibration	1	0.92	0.9	0.89		
Brake fluid	0.87	0.77	0.75	0.74	0.73	0.68
Motor oil	0.98	0.93	0.92	0.91	0.91	0.88
Battery acid	0.35	0.19	0.17	0.16		

[a]T = tension, and C = compression.

Table 4.5. Allowable stress intensity values, S_t (ksi) with bounding environmental and prior load effects (hot water and battery acid are not covered)

Temperature (°F)	Time						
	0 h	10 h	1000 h	3000 h	5000 h	1 year	15 years
–40	11.5	7.0	5.7	5.3	5.3	5.3	5.0
20	10.4	7.0	5.7	5.3	5.3	5.3	5.0
70	9.5	7.0	5.7	5.3	5.3	5.3	5.0
135	8.3	7.0	5.3	5.0	4.9	4.9	4.8
190	7.4	6.1	4.6	4.4	4.3		
250	6.2	4.3	3.1	2.9	2.9		

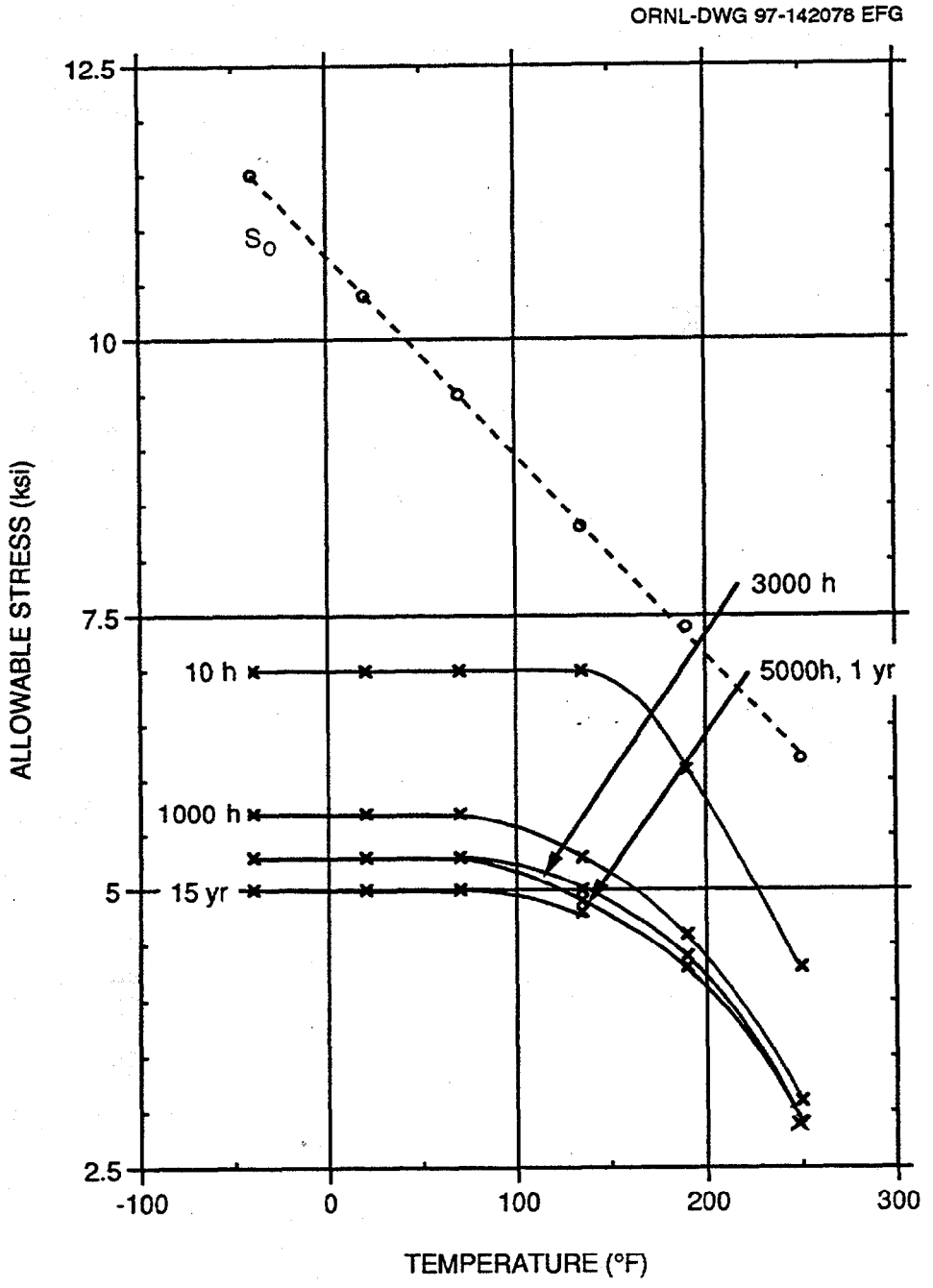

Fig. 4.2. S_t values with bounding environmental and prior loading effects.

The S_0 and S_t values establish limits on allowable in-plane membrane stress intensities, P. For out-of-plane bending away from geometric discontinuities, the membrane plus bending stress intensities, P + Q, are limited to

$$P + Q \leq 1.5\, S_t \,. \tag{4.3}$$

The flexure tests on which this higher limit is based are discussed in Chap. 3 of Part 2.

Geometric discontinuities include corners and bends. Here, the fiber distribution across the thickness of a composite plate or shell structure is likely to be less uniform. Even more importantly, when the inside surface of bends is in tension, a new failure mode (e.g., delaminations) is introduced (see Chap. 15 of Part 2). In these cases, the membrane plus bending stresses are limited as follows:

$$P + Q \leq 0.8\ S_t \text{ (at discontinuities)} \ . \tag{4.4}$$

4.3 TREATMENT OF INCREMENTS OF SUSTAINED LOADS

For changing stress levels, the time-fraction summation method shall be used to assess cumulative damage. The sum of the use fractions associated with the primary plus bending stresses for all increments of loading shall not exceed a value of 1.0.

$$\sum_i \left(\frac{t}{T_d} \right)_i \leq 1.0 \ . \tag{4.5}$$

Here, t_i is the specified duration of a given load increment i, and T_{d_i} is the allowable time for the stress intensity associated with that load increment.

REFERENCE

1. *Military Handbook Polymer Matrix Composites, Volume 1: Guidelines*, MIL-HDBK-17-1D, U.S. Department of Defense, February 1994.

5. DESIGN LIMITS FOR CYCLIC LOADINGS

5.1 BASIC FATIGUE DESIGN CURVES

Design fatigue curves are shown in Fig. 5.1. These curves are derived from average fatigue curves, as described in Chap. 11 of Part 2, by placing a margin of 20 on cycles to failure. This margin is believed to adequately cover data scatter, and, as shown in Chap. 10 of Part 2, it limits stiffness degradation during cycling to 10% or less, on average. The curves are applicable to temperatures over the range from –40 to 250°F. It is necessary only to multiply the ordinate, which is given as a percent of UTS, by the appropriate average UTS at the temperature of interest. The average room-temperature value is 21.3 ksi. At other temperatures UTS can be obtained by multiplying the room-temperature value by the appropriate factor from Fig. 2.1 or Table 2.1. Values are given in Table 5.1.

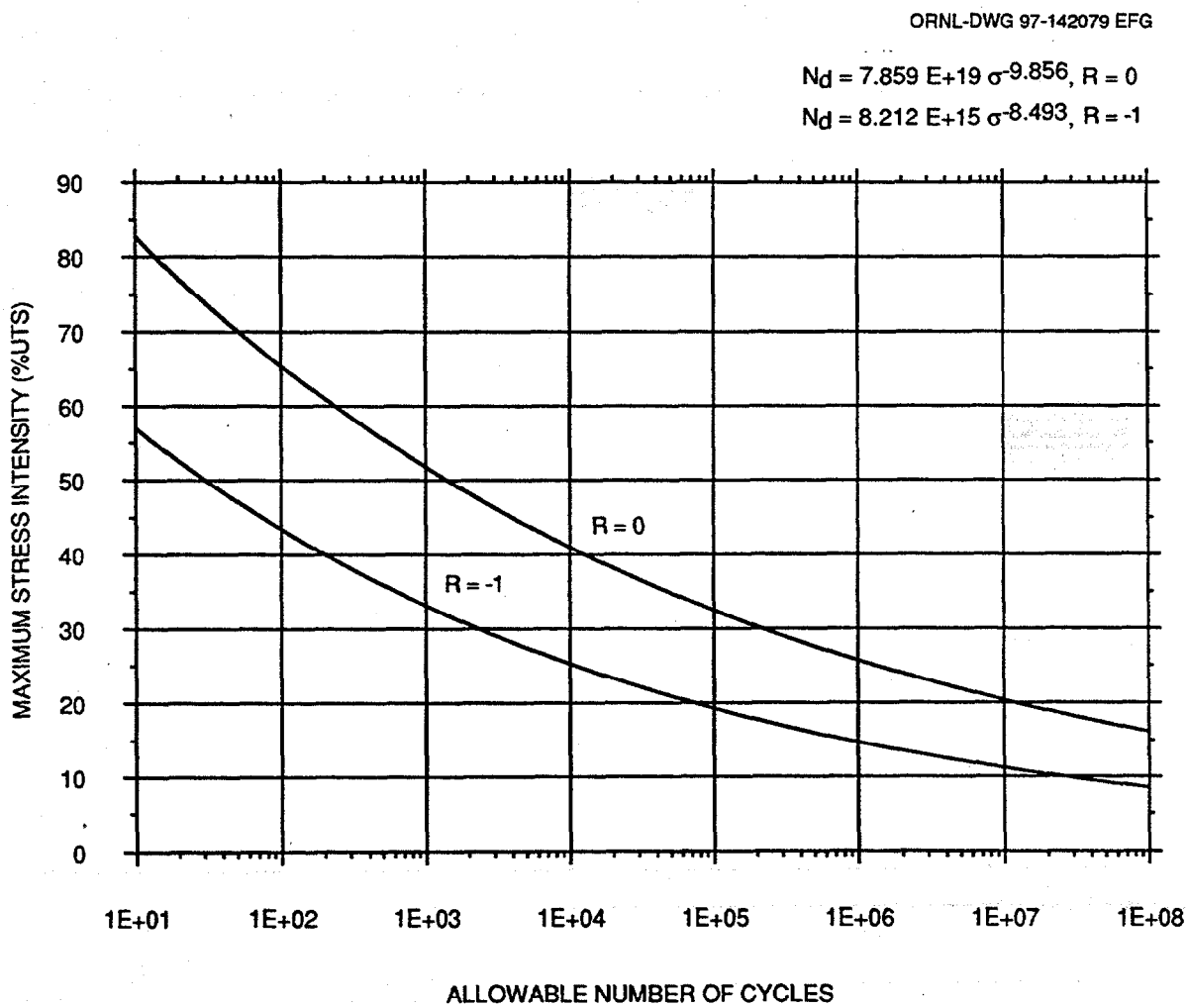

Fig. 5.1 Design fatigue curves. Curves are applicable to temperatures over range from –40 to 250°F when the normalized stress is multiplied by the *average* UTS at maximum temperature during the cycle.

Table 5.1. UTS at various temperatures

Temperature (°F)	Average 0° UTS (ksi)
–40	25.8
70	21.3
135	18.7
190	16.4
250	13.8

The curve labeled R = 0 in Fig. 5.1 is derived from tensile fatigue test data obtained at an R ratio (minimum stress in the cycle divided by maximum stress) of 0.1. It can be used directly to evaluate design cycles that have stresses alternating between zero and a maximum value.

The R = –1 curve in Fig. 5.1 is derived from completely reversed cyclic tests (zero mean stress). It can be used directly for design cycles that are completely reversed. It also is to be used to evaluate other cycles with a fixed mean stress, as described in the next section.

5.2 TREATMENT OF MEAN STRESSES

For cycles with a fixed mean stress, the mean stress effect is to be incorporated by a modified Goodman relation (see Chap. 11 of Part 2):

$$\sigma_a = \sigma_o\left(1 - \frac{\sigma_m}{\sigma_r}\right), \tag{5.1}$$

where

σ_a = the allowable stress amplitude for the cycle with a mean stress,
σ_o = the allowable stress amplitude (also maximum allowable cyclic stress) at the same number of cycles from the R = –1 curve in Fig. 5.1,
σ_m = mean stress in the cycle,
σ_r = the minimum creep-rupture strength, S_r, for the total time of the load cycles.

Values of $\sigma_r = S_r$ are plotted in Fig. 5.2. Conservatively, a σ_r value corresponding to 5000 h (the assumed longest vehicle operating time) may be used. Those values of σ_r are given in Table 5.2.

5.3 ENVIRONMENTAL EFFECTS

Table 5.3 gives environmental fatigue stress-reduction factors. These factors were obtained, as described in Chap. 11 of Part 2, from tests at R = 0.1. Specimens were presoaked in the indicated fluids for 100 h (with one exception) and then tested in the same fluid. These factors should be used to reduce the allowable design stress levels in Fig. 5.1.

A single factor of 0.7 for environmental effects covers everything except battery acid and the long-term hot water exposure and thus can be conservatively used.

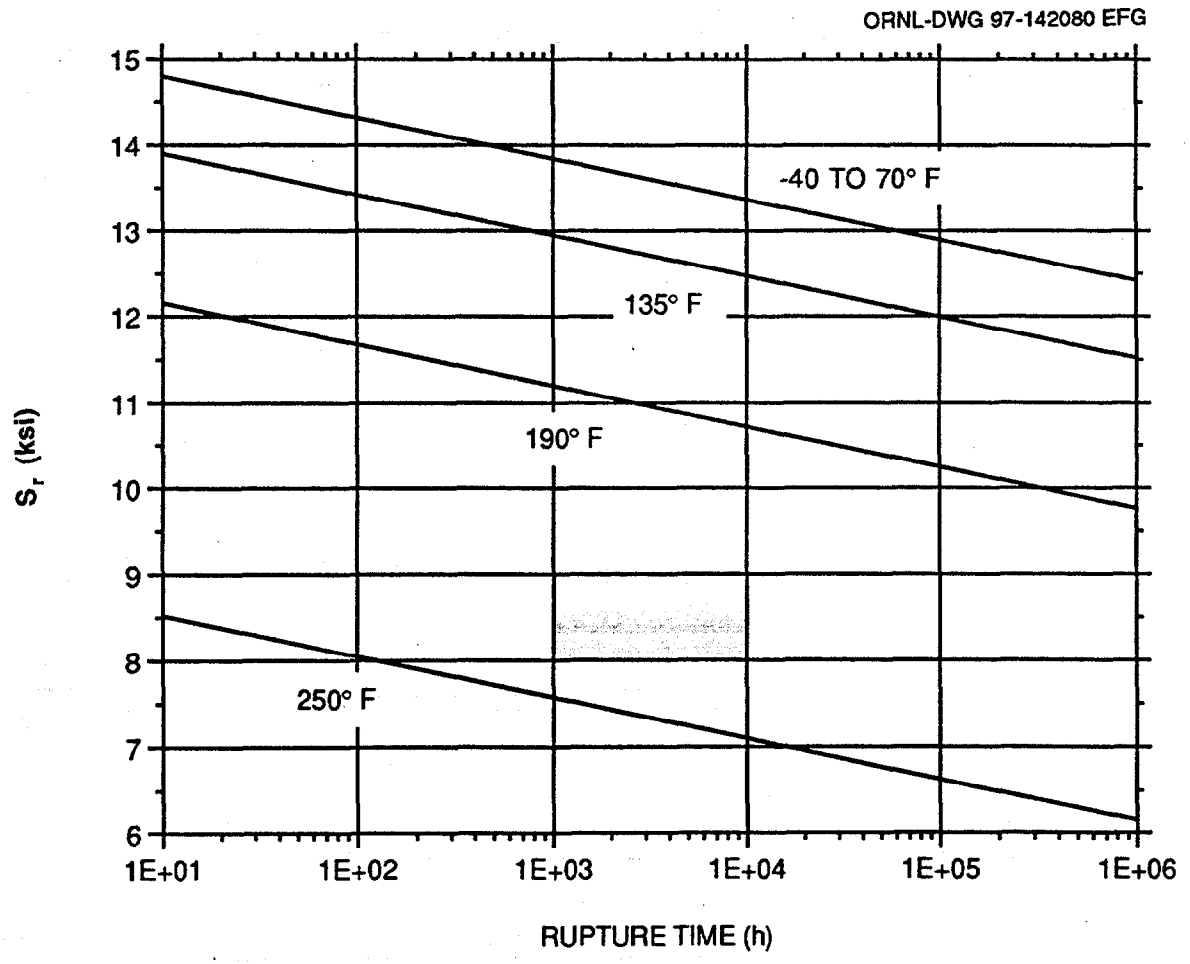

Fig. 5.2. Minimum creep-rupture stress values, S_r.

Table 5.2. σ_r at 5000 h for use in modified Goodman relation

Temperature (°F)	σ_r for 5000 h (ksi)
–40 to 70	13.5
135	12.6
190	10.9
250	7.3

Table 5.3. Fatigue stress-reduction factors for various automotive fluid environments

Fluid	Cycles			
	1×10^2	1×10^4	1×10^6	1×10^8
Air	1.00	1.00	1.00	1.00
Brake fluid	1.00	1.00	0.99	0.94
Motor oil	1.00	0.98	0.91	0.84
Engine coolant	1.00	1.00	0.87	0.71
Saltwater	1.00	0.95	0.86	0.78
Distilled water	0.95	0.90	0.85	0.81
Windshield wash	1.00	0.97	0.84	0.73
180°F water, 1080 h	0.64	0.69	0.74	0.80
Battery acid	1.00	0.73	0.50	0.34

5.4 TREATMENT OF VARYING STRESS AMPLITUDES

For varying stress amplitudes, Miner's rule should be used to account for cumulative fatigue damage (see Chap. 11 of Part 2). For a design to be acceptable, the fatigue damage should satisfy the following relation:

$$\sum_i \left(\frac{n}{N_d}\right)_i \leq 1.0 \ , \tag{5.2}$$

where n_i is the number of specified cycles for cycle type i and N_{d_i} is the number of design-allowable cycles for cycle i determined from one of the design fatigue curves (Fig. 5.1) corresponding to the maximum temperature of the cycle.

5.5 FATIGUE EVALUATION PROCEDURE

The following fatigue analysis procedure shall be used. For each cycle type, i, determine, for each point in the structure, the maximum stress intensity and, at a different time in the cycle, the minimum stress intensity. The algebraic difference between these two values yields the maximum possible stress range. The mean stress is the average of the two values, and the amplitude is one-half the stress range. The ratio R is formed by dividing the minimum stress intensity by the maximum stress intensity.

This procedure is not rigorous because the principal stress axes may rotate during the cycle. However, it is believed to be conservative because it results in the maximum stress intensity range.

The design fatigue curve corresponding to the maximum temperature of the cycle shall be used to determine N_d.

6. DAMAGE TOLERANCE DESIGN FOR LOW-ENERGY IMPACTS AND OTHER DEFECTS

6.1 GENERAL REQUIREMENTS

A two-part design assessment approach is recommended:

1. Assume the presence of a 0.25-in.-diam circular hole in the worst possible location of the structure. Analytically assess the structure with the hole. A calculated local stress concentration factor (SCF) greater than 1.1 need not be considered (see Chap. 14 of Part 2). However, the effects of the lost area must be taken into account. This evaluation will ensure that the structure can tolerate minor impacts and structural flaws at least up to a size of 0.25 in., no matter where they are located. The logic for this is discussed in Chap. 14 of Part 2.
2. For specified low-energy impacts such as roadway kickups, tool drops, and load drops in a pickup truck box, the procedures described in the following sections may be used to assess damage tolerance for damage areas larger than that corresponding to a 0.25-in.-diam hole.

6.2 DETERMINATION OF DAMAGE AREA

For a given object of mass, m, impacting the structure with a velocity, v, in the most highly stressed location, away from structural discontinuities, determine the impact damage from the "design" curve in Fig. 6.1. The design curve is the upper bound of test data generated from air-gun and pendulum impact tests on clamped 8-in.-diam by 1/8-in.-thick circular plates of the reference material. Development of this design curve and its applicability to real events, such as bricks dropped in a pickup box, are discussed in Chap. 13 of Part 2. The curve has been experimentally shown to cover a variety of variables, such as impactor size and mass variations, different environments (prior specimen soaks in water at various conditions and severe exposure to battery acid), and impacts at a temperature of –40°F.

As an alternative to the use of Fig. 6.1 to determine damage area, the following procedure involving dynamic structural analysis may be used. This procedure allows the characteristics of the impacting body and of the impacted structure to be taken into account. These characteristics are used in a thick-shell, dynamic time-response analysis, using a finite-element analysis program such as ABAQUS. Such an analysis provides the maximum contact force, which can be used with Fig. 6.2 to estimate the damage area. The basis of this approach is described in Chap. 13 of Part 2.

In the analytical procedure previously described, the local indentation behavior of the composite must be taken into account. The experimentally determined indentation behavior is shown in Chap. 13 of Part 2 to be governed by the classical Hertzian contact law:

$$F = K\alpha^{1.5} \ , \tag{6.1}$$

where F is the indentation force (lb), α is the indentation (in.), and K is an experimentally determined constant having a value of 17.0 for the reference composite. The Hertzian law is included in the analysis by attaching a nonlinear spring to the structure at the point of contact. The impacting object strikes the spring, which in turn transfers energy to the structure.

6.3 DETERMINATION OF STRENGTH AND STIFFNESS DEGRADATION

The damage area, predicted by one of the methods of Sect. 6.2, can either be factored into the structural evaluation as an equivalent circular hole, or the degradation in strength can be estimated as specified in the following paragraph. If the equivalent circular hole approach is used, a local SCF greater than 1.1 can be ignored (local stresses at the edge of the hole greater than 1.1× the average stress in that area). Stiffness degradation can best be estimated, conservatively, by the equivalent circular hole method.

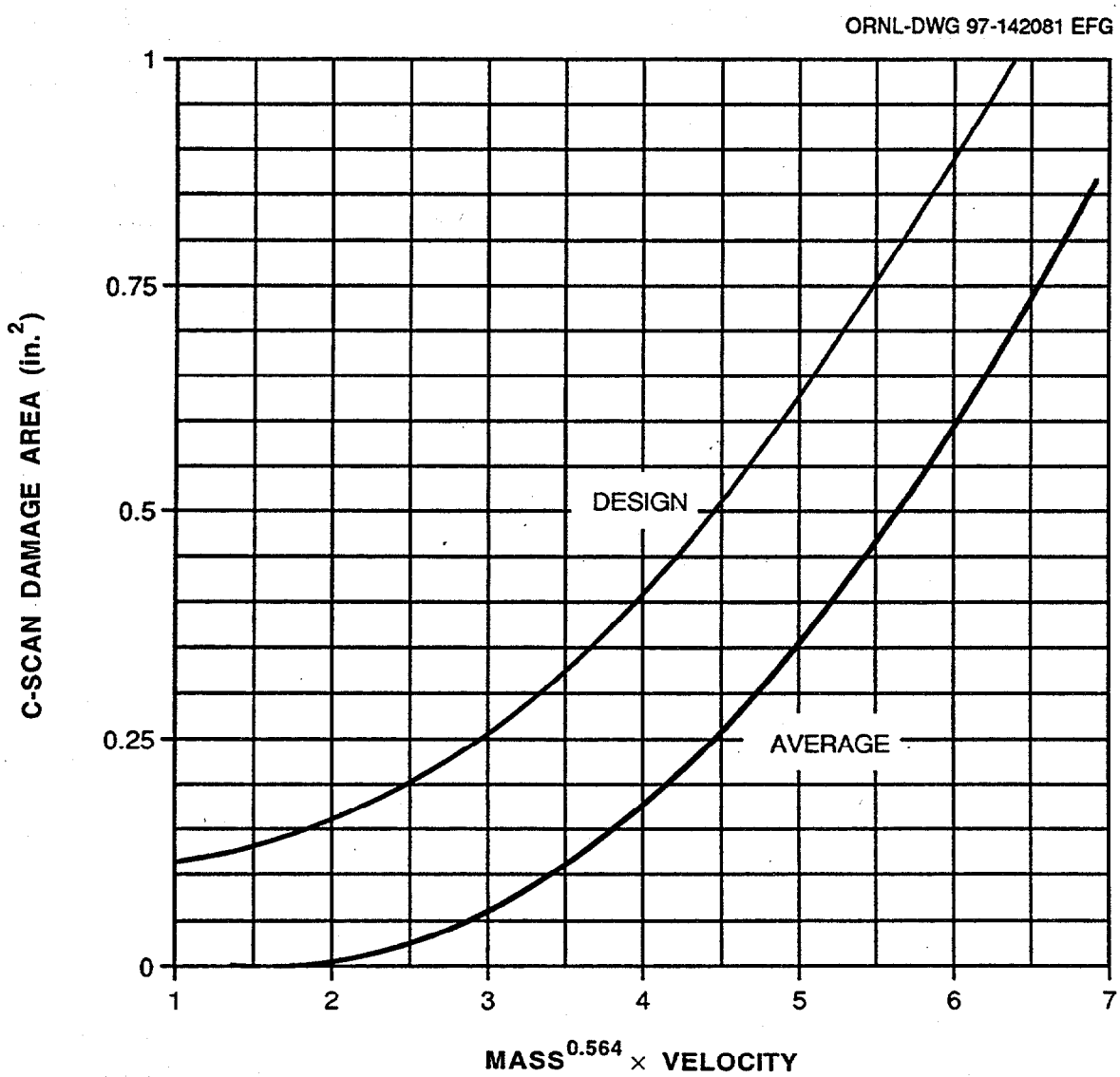

Fig. 6.1. Design curve for determining impact damage area. Mass is in lb-s^2/ft and velocity is in ft/s.

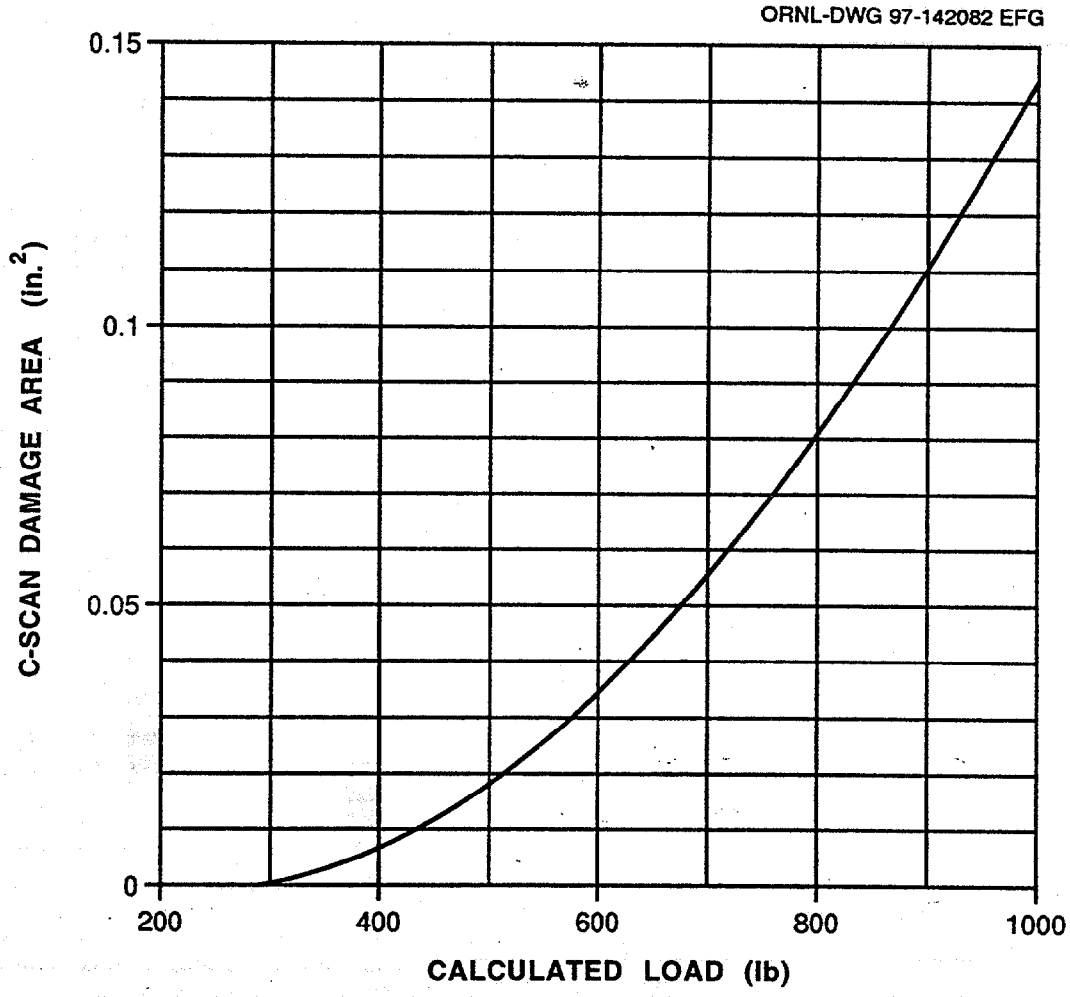

Fig. 6.2. Calculated peak contact force vs damage area. This figure should not be extrapolated beyond the limit shown.

For a given predicted damage area, the degradation in tensile, fatigue, and compressive strengths can be estimated using Fig. 6.3. These curves were derived from test data obtained from 1-in.-wide specimens cut from impacted plates. They show the strength of specimens containing the damage area relative to the strength in undamaged regions. The largest effect is in tension. In Chap. 14 of Part 2, it is shown that the tensile curve in Fig. 6.3 is essentially the same as would be predicted by representing the damage area as a circular hole and basing predicted failure on the average remaining ligament stress in the 1-in.-wide specimen. Clearly, in fatigue and compression the damaged area does contribute to strength. Use of an equivalent hole to estimate fatigue and compressive strength degradation would be conservative. In any event, in interpreting and using the results presented in Fig. 6.3, the fact that they are from tests of 1-in.-wide specimens should be considered.

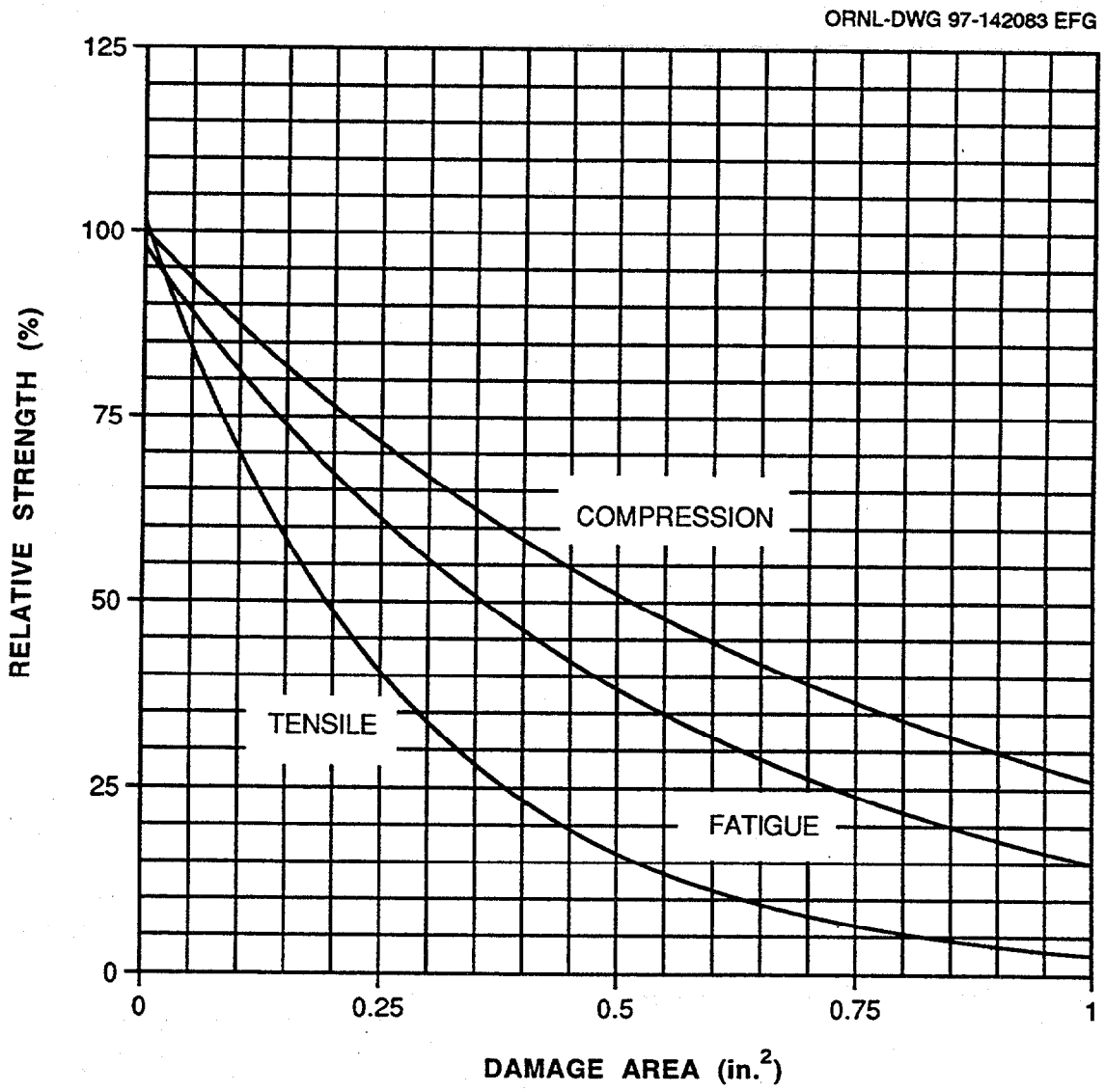

Fig. 6.3. Strength degradation as a function of damage area.

7. SUMMARY—SIMPLIFIED CRITERIA

This chapter briefly summarizes the scope of the detailed criteria presented in the previous chapters and condenses those criteria to a set of simplified rules consisting primarily of reduction factors on room-temperature, in-air, UTS, and stiffness values.

7.1 STIFFNESS AND CREEP PROPERTIES FOR DESIGN ANALYSES

Chapter 2 provides elastic constants and creep-strain relations for the CSM/isocyanurate reference composite based on the assumption of transverse isotropy (isotropic in the plane of the composite plaque). On this basis, only the elastic modulus and Poisson's ratio for the weaker 0° direction are used. Multipliers on the base room-temperature elastic modulus are given to account for temperature, environments, and prior load cycles. Likewise, a basic creep-strain equation is given for use in predicting time-dependent deformations, and factors are provided for accounting for temperature and environmental effects. These values and factors are summarized in simplified form in the following paragraphs.

The basic room-temperature elastic constants, Young's modulus and Poisson's ratio, are $E = 1.37$ Msi and $\nu = 0.31$. Multipliers on E to account for temperature are given in Table 7.1.

To conservatively account for prior cyclic loadings, E values determined by the multipliers in Table 7.1 should be multiplied by 0.90. To conservatively account for environment, a further multiplication of E by 0.83 is required.

Creep, for a given time under load, can be approximately accounted for by using a reduced time-dependent "elastic modulus" in an elastic analysis. Values of these reduced moduli for key times at room temperature are tabulated in Table 7.2.

Table 7.1. Temperature multipliers for modulus of elasticity

Temperature (°F)	Multiplier on E
–40	1.21
70	1.00
135	0.88
190	0.77
250	0.65

Table 7.2. Time-dependent modulus values

Time under load	Time-dependent modulus, E_t (Msi)
10 h	1.24
3000 h	1.03
5000 h	1.00
15 years	0.81

The factors in Table 7.3 can be used to conservatively convert the room-temperature modulus values in Table 7.2 to values for other temperatures.

Table 7.3. Temperature multipliers for time-dependent moduli

Temperature (°F)	Multiplier on E_t
–40	1.21
70	1.00
135	0.81
190	0.66
250	0.53

To conservatively account for environment, an additional multiplier of 0.63 should be applied to E_t.

7.2 MULTIAXIAL STRENGTH THEORY

It is shown in Chap. 3 that the maximum shear stress theory of failure, when based just on the UTS in the weaker 0° direction, conservatively predicts failures for other in-plane stress states and directions—biaxial tension, compression, and shear. By defining an equivalent intensity of combined stresses, or stress intensity, at a point as twice the maximum shear stress, the predicted stress intensity can simply be compared to uniaxial tensile allowable stresses. The predicted stress intensity is the difference between the algebraically largest principal stress and the algebraically smallest principal stress at a point. Tensile stresses are considered positive, and compressive stresses are considered negative.

7.3 ALLOWABLE STRESSES FOR STATIC LOADINGS

Both time-independent and time-dependent allowable stress intensities are given in Chap. 4, the former for short-time operating loads and the latter for longer-time sustained loads. The time-independent allowable, S_0, is defined as

$$S_0 = 2/3\ UTS_{min}\ ;$$

and the time-dependent allowable is defined as 0.8 S_r, where S_r is the minimum creep-rupture strength. A single set of allowables, S_t, covering times from 0 to the 15-year design life of a vehicle is established as follows:

$$S_t \leq \begin{cases} S_0 \\ 0.8\, S_r \end{cases} .$$

Values of S_t over the design temperature range of –40 to 250°F are given in Chap. 4. Reduction factors are given for the effects of environments and prior cyclic loadings, and S_t values that include the reductions are also tabulated.

The calculated in-plane membrane stress intensities, P, are limited to $P \leq S_t$. The membrane plus out-of-plane bending stress intensities, P + Q, are limited to $P + Q \leq 1.5\ S_t$ away from geometric discontinuities. At bends and corners, the limit is $P + Q \leq 0.8\ S_t$.

For changing stress levels, the time-fraction summation method shall be used:

$$\sum_i \left(\frac{t}{T_d}\right)_i \leq 1.0 \ .$$

Here, t_i is the specified duration of a given load increment, i, and T_{d_i} is the allowable time for the stress intensity associated with that load increment.

The minimum room-temperature UTS value for the 0° direction of the reference composite is 17.4 ksi. With this value, S_0 is 11.6 ksi at room temperature. Table 7.4 gives the S_t values as multipliers on the room-temperature allowable stress, S_0.

Table 7.4. S_t values expressed as multipliers on S_0 at room temperature

Temperature	Time						
(°F)	0 h	10 h	1000 h	3000 h	5000 h	1 year	15 years
–40	1.22	1.03	0.96	0.94	0.93	0.92	0.89
20	1.09	1.03	0.96	0.94	0.93	0.92	0.89
70	1.00	1.00	0.96	0.94	0.93	0.92	0.89
135	0.88	0.88	0.88	0.88	0.87	0.86	0.83
190	0.78	0.78	0.78	0.76	0.75		
250	0.66	0.59	0.52	0.51	0.50		

The 0-h S_0 multipliers in Table 7.4 should be reduced by the factor 0.82 to account for environment and prior cyclic loading. The time-dependent values in the table can conservatively be multiplied by 0.49 to account for environment and prior cyclic loading.

7.4 LIMITS FOR CYCLIC LOADINGS

Chapter 5 presents design fatigue curves for two types of cycles: R = 0 and R = –1, where R is the ratio of the minimum to maximum stress intensity in the cycle. Stress is expressed as a percent of the average UTS; the curves apply to any temperature over the –40 to 250°F range, if UTS at that temperature is used. A modified Goodman relation is used to conservatively account for mean stresses, and factors are provided to account for environmental effects:

$$\sigma_a = \sigma_o \left(1 - \frac{\sigma_m}{\sigma_r}\right) .$$

Here, σ_a is the allowable stress amplitude for the cycle with a mean stress, σ_o is the allowable stress amplitude from the R = –1 design curve, σ_m is the mean stress, and σ_r is the minimum creep-rupture strength for the total time of cyclic operation (see Table 5.2).

Miner's rule is used to account for cycles of different stress amplitudes:

$$\sum_i \left(\frac{n}{N_d}\right)_i \leq 1.0 \ ,$$

where n_i is the number of cycles of type i and N_d is the number of design allowable cycles of type i.

Maximum allowable cyclic stress values from the design fatigue curves are given in Table 7.5.

Table 7.5. Maximum allowable cyclic stresses as a percent of UTS_{avg}

Load ratio, R	Stress (% UTS_{avg})			
	10^2 cycles	10^4 cycles	10^6 cycles	10^8 cycles
0	65.4	41.0	25.7	16.1
−1	43.5	25.3	14.7	8.5

The average UTS in the 0° direction of the reference material is 21.3 ksi. The multipliers given in Sect. 7.1 to account for the effects of temperature on stiffness, E, also apply to strength and should be used to determine UTS_{avg} at other temperatures. An environmental factor of 0.7 on stress covers all environments except battery acid.

7.5 DAMAGE TOLERANCE EVALUATION

Chapter 6 recommends a two-part design assessment approach for evaluating damage from low-energy impacts and small flaws from other sources. First a 0.25-in.-diam circular hole in the worst possible location of the structure should be assumed and its effects on structural strength and stiffness evaluated via analysis (a local stress concentration factor greater than 1.1 can be ignored). This evaluation will ensure that the structure can tolerate minor impacts and structural flaws up to a size of 0.25 in.

For specific low-energy impacts such as roadway kickups, tool drops, and load drops in a pickup box, experimentally derived correlations are given for (1) conservatively estimating the damage area from the mass and velocity of the impacting object and (2) determining, from the estimated damage area, the degradation in tensile strength, compressive strength, and fatigue strength. The correlations provided are believed to adequately include the effects of environments and temperature.

For a given damage area, the tensile strength degradation is considerably larger than that for compressive or fatigue strengths. Further, the tensile strength degradation can be determined by assuming that the damage area is a circular hole of equivalent area.

Table 7.6 shows specific values taken from the graphical correlations (Figs. 6.1 and 6.3) in Chap. 6.

Table 7.6. Predicted effect of low-energy impacts[a]

$m^{0.564}v$	Damage area (in.^{2})	Tensile strength degradation factor[b]
1.0	0.12	0.67
2.0	0.16	0.57
3.0	0.26	0.40
4.0	0.41	0.23
5.0	0.63	0.10
6.0	0.89	0.04

[a]The quantity m is mass (lb-s^2/ft), and v is velocity (ft/s).

[b]These strength reduction factors apply only to a 1-in.-wide specimen. They are essentially the tensile strength reductions caused by the net area being reduced by a circular hole of equivalent area.

INTERNAL DISTRIBUTION

1. R. L. Battiste
2. H. W. Blake
3. R. G. Boeman
4. C. R. Brinkman
5–14. J. M. Corum
15. W. G. Craddick
16. M. Elahi
17. D. L. Erdman
18. J. G. Hansen
19. H. W. Hayden, Jr.
20. W. K. Kahl
21. L. D. Klett
22. C. R. Luttrell
23. R. N. McGill
24. D. J. Naus
25. R. E. Norris
26. W. Ren
27. M. B. Ruggles
28. W. A. Simpson, Jr.
29. P. A. Sklad
30. J. M. Starbuck
31. C. D. Warren
32. Y. J. Weitsman
33. G. T. Yahr
34. T. Zacharia
35. R. E. Ziegler
36. ORNL Patent Section
37. Laboratory Records, ORNL-RC
38-39. Laboratory Records, OSTI

EXTERNAL DISTRIBUTION

40. R. S. Benson, Department of Materials Science and Engineering, The University of Tennessee, 427-C Dougherty Engineering Building, Knoxville, Tennessee 37996-2200.
41. R. A. Bergen, MSX International, 255 Rex Boulevard, Auburn Hills, Michigan 48326.
42. K. Fielder, The Dow Chemical Company, 2301 N. Brazosport Blvd., B-1608, Freeport, Texas 77541-3257.
43. R. B. Freeman, The Budd Company, 1515 Atlantic Boulevard, Auburn Hills, Michigan 48326.
44. R. Gjerde, Textron Automotive Company, 100 Brady Road, Americus, Georgia 31709.
45–74. E. M. Hagerman, Automotive Composite Consortium, General Motors, 30500 Mound Road, I-6, Box 9055, Warren, Michigan 48090-9055.
75. J. M. Henshaw, Department of Mechanical Engineering, The University of Tulsa, 600 S. College Avenue, Tulsa, Oklahoma 74104-3189.
76. G. A. Holmes, National Institute of Standards and Technology, Bldg. 224, Room B116, MS: Room B108, Gaithersburg, Maryland 20899.
77. D. Kossak, Cambridge Industries, 29333 Stephenson Highway, Madison Heights, Michigan 48071.
78. F. G. Krautz, Vetrotex Certainteed, 4515 Allendale Road, Wichita Falls, Texas 76310-2199.
79. P. K. Liaw, Department of Materials Science and Engineering, The University of Tennessee, 427-B Dougherty Engineering Building, Knoxville, Tennessee 37996-2200.
80. K. Liechti, Engineering Mechanics Research Laboratory, Department of Aerospace Engineering and Engineering Mechanics, The University of Texas at Austin, Austin, Texas 78712.
81. G. R. Miesel, Ashland Chemical Company, 900 Wilshire Drive, Suite 110, Troy, Michigan 48084.
82. L. M. Ojanen, Decona International, 50 Casmir Court, Concord, Ontario, Canada L4K 4J5.
83. D. Oplinger, AAR-431, FAA William J. Hughes Technical Center, Atlantic City International Airport, New Jersey 08405.
84. T. A. Reinhart, The University of Dayton Research Institute, 300 College Park Drive, Dayton, Ohio 45469-0130.
85. D. N. Robinson, Department of Civil Engineering, The University of Akron, Akron, Ohio 44325-3905.

86. G. Sandgren, Owens Corning Science & Technology Centre, 2790 Columbus Road, Route 16, Granville, Ohio 43023-1200.
87. C. R. Schultheisz, National Institute of Standards and Technology, Building 224, Room A209, Gaithersburg, Maryland 20899.
88. T. D. Seagrave, Bayer Corporation, 100 Bayer Road, Pittsburgh, Pennsylvania 15205.
89. L. V. Smith, Washington State University, School of Mechanics and Materials Engineering, Pullman, Washington 99164-2920.
90. C. T. Sun, Purdue University, School of Aeronautics and Astronautics, 1282 Grissom Hall, West Lafayette, Indiana 47907-1282.
91. R. Talreja, School of Aerospace Engineering, Georgia Institute of Technology, Atlanta, Georgia 30332-0150.
92. D. C. Worley, Department of Materials Science and Engineering, The University of Tennessee, 427-B Dougherty Engineering Building, Knoxville, Tennessee 37996-2200.

93–95. J. A. Carpenter, U.S. Department of Energy, 1000 Independence Avenue, SW, Washington, DC 20588.

96. H. E. Clark, U.S. Department of Energy, Oak Ridge Site Office, Oak Ridge, Tennessee 37831.
97. P. G. Patil, U.S. Department of Energy, 1000 Independence Avenue, SW, Washington, DC 20588.
98. M. R. Rawlins, U.S. Department of Energy, Oak Ridge Site Office, Oak Ridge, Tennessee 37831.